Alberti, M., et al., 2020, Stress in the tropics? Impact of a latitudinal seawater 18O gradient on Middle Jurassic temperature reconstructions at low latitudes: Geology, v. 48, https://doi.org/10.1130/G47824.1

Material

The present study combines new stable oxygen isotope data from Morocco, Tunisia, Israel, and Jordan with already published results from Egypt (Alberti et al., 2017). The geographic coordinates of the individual study areas are listed in Table S1.

Previous reconstructions of absolute water temperatures for the Jurassic of Europe are dominated by stable oxygen isotope analyses of belemnite rostra (e.g., Dera et al., 2011; Martinez and Dera, 2015; Korte et al., 2015). However, these fossils generally record more positive $\delta^{18}O$ values than co-occurring bivalve and brachiopod shells. The reason for this discrepancy is not yet completely known, but some authors consider belemnite rostra to be less reliable for temperature reconstructions (compare Mutterlose et al., 2010; Alberti et al., 2012a, b; Price et al., 2015; Hoffmann and Stevens, 2019). More recent studies suggest that the fractionation factor for stable oxygen isotopes in belemnites from seawater was closer to that of abiogenic calcite compared to other marine organisms (Vickers et al., 2020). If this is true, temperatures reconstructed with belemnite rostra would be considerably higher. Due to these problems and because belemnites are relatively uncommon in most of the Middle and Upper Jurassic strata of northern Africa and western Asia, the current study uses calcitic shells of bivalves and rhynchonellid brachiopods.

Only very few fossil shells were available for analyses from the Jurassic of Morocco collected during a field survey by F.T. Fürsich in March-April 1990. These specimens were collected from the ?Toarcian-Aalenian south of Ifri, the Bajocian south of Feggou, the Callovian south of Imouzèr-des-Ida-Outanane, and the Oxfordian east of Smimou. All these outcrops are part of the Atlas Mountains System. The shells include rhynchonellid brachiopods as well as the oysters *Nanogyra nana*, *Exogyra chouberti*, and *Gryphaea* sp. Unfortunately, no precise age assignments beyond stage level were possible.

Jurassic fossils of southern Tunisia were collected for palaeoecologic analyses by S. Holzapfel (1998) and her material is stored in the Bayerische Staatssammlung für Paläontologie und Geologie in Munich, Germany. In the present study, 41 well-preserved rhynchonellid brachiopod shells from seven Callovian sections close to and south of Tataouine were analysed. Each shell could be attributed to a particular horizon in the sections measured by Holzapfel (1998), but the scarcity of ammonites in the succession does not allow very precise age assignments beyond substage level. The sampled horizons belong to the Beni Oussid, Krechem el Miit, and Ghomrassen members of the Tataouine Formation. The Beni Oussid and Krechem el Miit members are characterized by alternations of marl, carbonates, silt- and sandstones, while the lower Ghomrassen Member consists of pack- and grainstones (Holzapfel, 1998). The sampled levels are characterized by a highly diverse fauna (including irregular echinoids and nautiloids) pointing to fully marine conditions on a carbonate platform (Holzapfel, 1998).

Fossils from the Middle to Upper Jurassic of Gebel Maghara in the Sinai of northeastern Egypt were collected for palaeontological studies by A.A. Abdelhady (2014; Abdelhady and Fürsich, 2014, 2015a, b, c). This material is currently stored at the GeoZentrum Nordbayern of the Friedrich-Alexander-Universität Erlangen-Nürnberg, Germany. The stable isotope ($\delta^{18}O$) composition of 73 well-preserved shells with Bajocian to Kimmeridgian ages was analysed (Alberti et al., 2017). Biostratigraphic studies allowed the assignment of ammonite zones to the individual samples (Abdelhady and Fürsich, 2015a). The stable isotope data is presented here with an improved stratigraphic resolution, but for more details see the earlier study (Alberti et al., 2017).

Thirty-five well-preserved rhynchonellid brachiopods and oysters were collected by M. Alberti and Y. Leshno from the Middle Jurassic and Lower Cretaceous of the Negev Desert of southern Israel during a field survey in November 2017. Two brachiopods could be found in the Upper Bajocian Mahmal Formation of Makhtesh Ramon, 29 shells were collected from the Callovian Zohar and Matmor formations of the Makhtesh Gadol, and four oysters stem from the Lower Cretaceous of Makhtesh Ramon. The Jurassic material could be assigned to earlier defined subunits (Goldberg, 1963; Parnes, 1981; Hirsch, 2005). Unfortunately, the general scarcity of ammonites complicates biostratigraphic dating for most of the Jurassic succession and only the Callovian specimens could be assigned to ammonite zones. While large parts of the Jurassic of southern Israel are nearly unfossiliferous, the Callovian strata of the Makhtesh Gadol contain an abundant fully marine fauna

Table S1 Approximate geographic coordinates of the sampled sections in this study.

No.	Locality	Latitude	Longitude
MO-1	Morocco (~1 km S of Ifri)	N 31.272	W 6.072
MO-2	Morocco (~1.5 km S of Feggou; precise locality unknown)		
MO-3	Morocco (~10 km S of Imouzér-des-Ida-Outanane)	N 30.620	W 9.400
MO-4	Morocco (~12 km E of Smimou)	N 31.208	W 9.579
TU-1	Tunisia (15 Remada Southeast)	N 32.250	E 10.545
TU-2	Tunisia (14 Faljet Jdari / Ed- Dghaghra)	N 32.462	E 10.426
TU-3	Tunisia (13 Krechem el Miit)	N 32.617	E 10.400
TU-4	Tunisia (12 Bir Remtha)	N 32.735	E 10.478
TU-5	Tunisia (11 Ksar Beni Soltane; Tazerdunet)	N 32.790	E 10.515
TU-6	Tunisia (5 Foum Tataouine Poste Optique)	N 32.970	E 10.450
TU-7	Tunisia (4 Foum Tataouine North)	N 33.045	E 10.380
EG-1	Egypt (Gebel Maghara-Homayir)	N 30.647	E 33.328
EG-2	Egypt (Gebel Maghara-Arousiah)	N 30.677	E 33.355
EG-3	Egypt (Gebel Maghara-Engabashi)	N 30.698	E 33.387
EG-4	Egypt (Gebel Maghara-Mowerib)	N 30.682	E 33.422
IS-1	Israel (Makhtesh Gadol; gad-11)	N 30.948	E 35.000
IS-2	Israel (Makhtesh Gadol; gad-43)	N 30.941	E 34.983
IS-3	Israel (Makhtesh Gadol; gad-47)	N 30.941	E 34.982
IS-4	Israel (Makhtesh Gadol; gad-48)	N 30.941	E 34.981
IS-5	Israel (Makhtesh Gadol; gad-60/61)	N 30.942	E 34.980
IS-6	Israel (Makhtesh Gadol; gad-62)	N 30.943	E 34.980
IS-7	Israel (Makhtesh Gadol; gad-63)	N 30.943	E 34.980
IS-8	Israel (Makhtesh Ramon; ram-5a; 15-01)	N 30.627	E 34.842
IS-9	Israel (Makhtesh Ramon; ram-5a; 15-02)	N 30.617	E 34.836
IS-10	Israel (Makhtesh Ramon; ram-Cr)	N 30.624	E 34.842
JO-1	Jordan (Wadi Nimr)	N 32.108	E 35.660
JO-2	Jordan (Arda)	N 32.125	E 35.654
JO-3	Jordan (Wadi Huni)	N 32.175	E 35.705
JO-4	Jordan (Tal el Dhahab)	N 32.189	E 35.713
JO-5	Jordan (King Talal Dam)	N 32.191	E 35.800

including echinoids, brachiopods, and occasional ammonites.

Jurassic fossils in northern Jordan were collected for palaeoecologic and taxonomic studies by F. Ahmad (1999) and his material is stored in the Bayerische Staatssammlung für Paläontologie und Geologie in Munich, Germany. Thirty bivalve shells from five sections northwest of Amman were analysed in the present study. The material can be attributed to horizons with Bajocian, Bathonian, and Callovian ages, but the general lack of ammonites in the sections hinders more precise age assignments beyond stage level (Ahmad, 1999). Lithostratigraphically, the fossils represent the Dhahab, Ramla, Hamam, and Mughanniyya formations.

Illustrations of the analysed species can be found readily in already published articles (Dubar, 1967; Holzapfel, 1998; Ahmad, 1999; Feldman et al., 2001, 2012, 2014; Alberti et al., 2017).

Palaeolatitudes

Palaeolatitudes were reconstructed with the help of the so-called Paleolatitude Calculator developed by van Hinsbergen et al. (2015) and using the palaeomagnetic reference curves of Kent and Irving (2010) for Morocco and Torsvik et al. (2012) for the other study areas. Due to a slight clockwise rotation of Africa, Morocco was situated at a much more northern position compared to Jordan during the Jurassic. Within the present study, palaeolatitudes are usually rounded to integers, but in the tables and figures values with one decimal are given. It has to be noted, however, that the reconstruction of palaeolatitudes is not a very precise science and absolute values can differ considerably among different studies. The given values are therefore mathematical and some degree of error has to be tolerated. Nevertheless, even changes of a few degrees in latitude for the different study sites would not influence the overall shape of the reconstructed latitudinal temperature gradients or the approximated $\delta^{18}O_{sea}$ values. Although the exact locality of the sampling site near Feggou in Morocco is unknown, a palaeolatitude of 27.1 °N was determined for the general study area in the Bajocian.

Preservation of fossil shells

A thorough check of the preservational quality of fossils used for stable isotope analyses is a fundamental step in producing reliable temperature data. In this context, cathodoluminescence microscopy has become a standard method to select suitable specimens and sampling areas (e.g., Wierzbowski, 2002, 2004; Ullmann and Korte, 2015; Arabas, 2016). Only shells with large non-luminescent areas pointing to a good preservation were used to reconstruct water temperatures in the present study (Fig. S1A-C). Furthermore, selected fossils were studied with a scanning electron microscope, which was particularly helpful in examining the fine microstructure of rhynchonellid brachiopods (Fig. S1D-F). For some fossils from Jordan (with the lowest palaeolatitudes in the dataset), enough carbonate powder could be extracted to also measure Mg/Ca- and Sr/Ca-ratios as well as manganese and iron contents. Shells with an original, unaltered chemical composition are believed to have very low manganese and iron contents (e.g., Price and Sellwood, 1997; Wierzbowski and Joachimski, 2007; Wierzbowski et al., 2009). Consequently, eight specimens were excluded from temperature reconstructions, because they contained more than 300 µg/g iron and/or more than 100 µg/g manganese (comparable to cut-off-values used by Alberti et al., 2012a, b). Another commonly mentioned indicator for the diagenetic alteration of fossil shells in a collection is a strong, positive correlation between their $\delta^{18}O$ and $\delta^{13}C$ values, since both values generally decrease progressively with increased alteration (compare Hodgson, 1966; Hudson, 1977; Nelson and Smith, 1996). This effect can be seen very well in the sediment and cement samples which commonly show lower $\delta^{18}O$ and $\delta^{13}C$ values than the seemingly well-preserved shells (Fig. S2A). While the number of specimens from Morocco is too small to examine a possible relationship between their $\delta^{18}O$ and $\delta^{13}C$ values, there is no statistically significant correlation in the results from Tunisia (rs = 0.22; p =

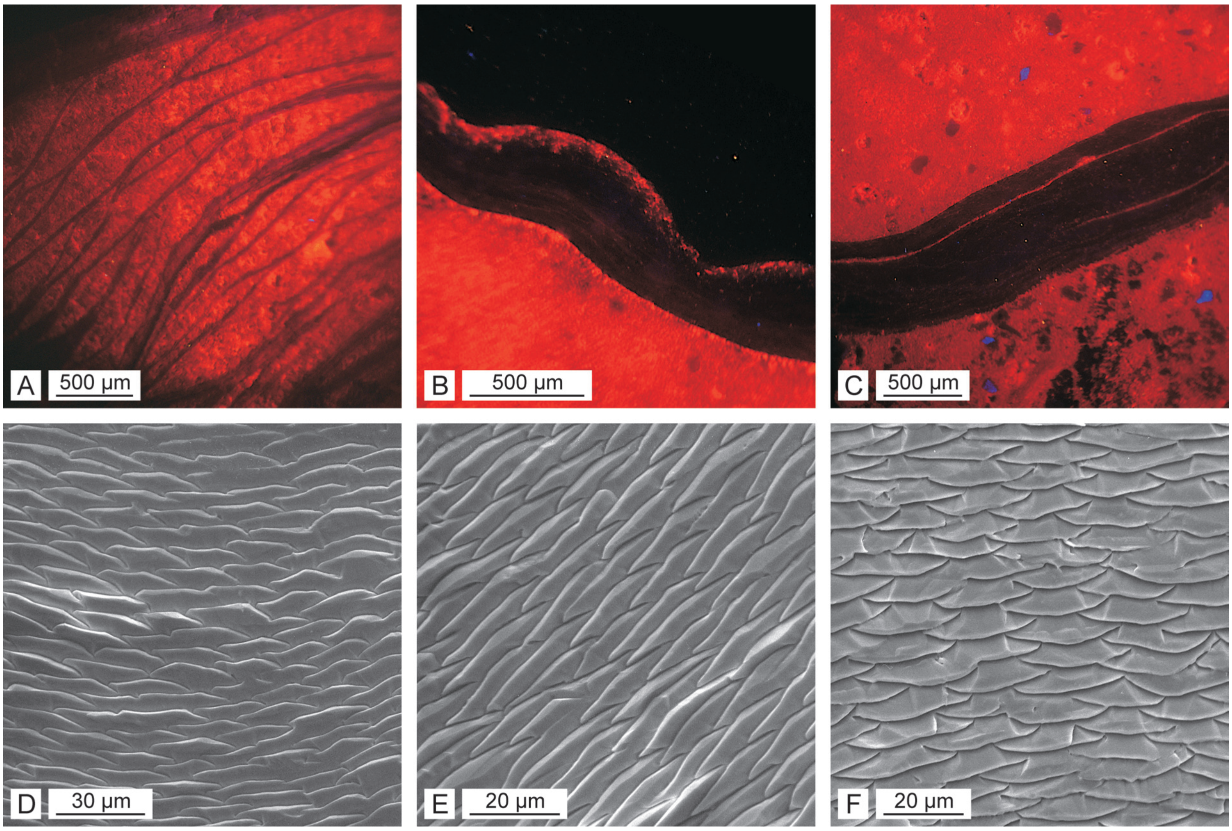

Fig. S1 Cathodoluminescence and scanning electron microscopy. The specimens were cut into slabs with their surface ground. Scanning electron microscopy was conducted after etching of the fossils with 5 % HCl for ca. 40 s. **A.** Poorly preserved gryphaeid oyster with sparry calcite filling voids within the shell (Jurassic, Morocco). **B.** Well-preserved specimen of *Somalirhynchia* cf. *africana* showing a luminescent outer shell margin due to weathering and possibly bioerosion (Callovian, Tunisia). **C.** Luminescent cracks in an otherwise well-preserved shell of *Septirhynchia pulchra* (Callovian, Tunisia). **D-F.** Specimens of *Somalirhynchia* cf. *africana* (D), *Daghanirhynchia angulocostata* (E), and *Somalirhynchia smelliei* (F) exhibiting well-preserved shell microstructure (Callovian, Tunisia).

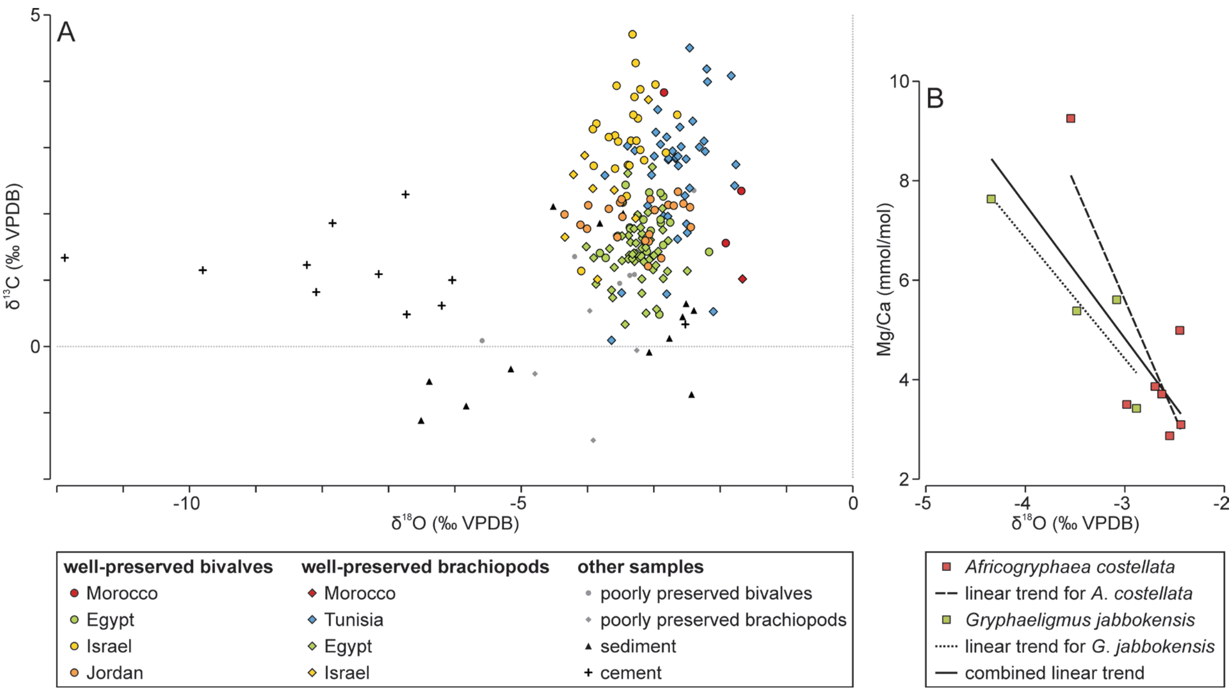

Fig. S2 A. $\delta^{18}O$ versus $\delta^{13}C$ values of well-preserved bivalves and brachiopods compared to results from poorly-preserved shells, sediment and cement. **B.** $\delta^{18}O$ values versus Mg/Ca-ratios of well-preserved shells of *Africogryphaea costellata* and *Gryphaeligmus jabbokensis* from Jordan.

0.17), Egypt (rs = 0.11; p = 0.36), and Jordan (rs = 0.17; p = 0.44). The data from Israel show a weak positive correlation (rs = 0.51; p = 0.002), which is not conclusive. Nevertheless, since the absolute $\delta^{18}O$ and $\delta^{13}C$ values of shells from Israel are comparable to those of Jordan and Egypt, it can be assumed that they are not altered. Summarizing the studies examining the preservational quality of the analysed shells, it seems plausible that the specimens used for temperature reconstructions are well preserved and show a pristine chemical composition.

Geochemical analyses

The selected fossils were sampled with a hand-held dental drill in the case of thick shells or with a computer-controlled micromill. Areas near the umbo/hinge as well as the muscle scar were avoided for bivalve shells (compare Huyghe et al., 2020). Similarly, rhynchonellid brachiopod shells were preferentially sampled in the center of the shells avoiding the umbo/pedical opening. The retrieved carbonate powder (0.05-0.50 mg) was then analysed using a carbonate preparation device (Kiel IV) connected with a ThermoScientific MAT 253 mass spectrometer at the Leibniz Laboratory for Radiometric Dating and Stable Isotope Research at the Christian-Albrechts-Universität zu Kiel, Germany. The samples were reacted within the preparation device with 100 % H_3PO_4 at 75 °C and the evolved CO_2 gas was analysed using the mass spectrometer. On a daily routine, different laboratory internal carbonate standards and two international carbonate standards were analysed to control the precision of measured $\delta^{13}C$ and $\delta^{18}O$ values. As documented by the performance of international [NBS19: +1.95 ‰ VPDB (^{13}C), -2.20 ‰ VPDB (^{18}O); IAEA-603: +2.46 ‰ VPDB (^{13}C), -2.37 ‰ VPDB (^{18}O)] and laboratory-internal carbonate standards [Hela1: +0.91 ‰ VPDB (^{13}C), +2.48 ‰ VPDB (^{18}O); HB1: -12.10 ‰ VPDB (^{13}C), -18.10 ‰ VPDB (^{18}O); SHK: +1.74 ‰ VPDB (^{13}C), -4.85 ‰ VPDB (^{18}O)], analytical precision of stable isotope analysis is better than ±0.08 ‰ (±1SD) for $\delta^{18}O$ and better than ±0.05 ‰ (±1SD) for $\delta^{13}C$. All values are reported in per mil relative to the Vienna Pee Dee Belemnite (VPDB) scale using NBS-19.

Trace element contents and molar Sr/Ca and Mg/Ca ratios of the bivalve shells of Jordan were determined by ICP-Optical Emission Spectrometry (ICP-OES) using a Ciros SOP instrument (Spectro Analytical Instruments, Germany) at the Institute of Geosciences, Christian-Albrechts-Universität zu Kiel. Sample introduction was via a concentric micro-nebulizer (GE SeaSpray 400µL) combined with a temperature-controlled cyclonic spray chamber. Typical sample weights for dissolution with 0.3 molar nitric acid were between 0.01 and 0.6 mg, and the final solution ready for analysis was adjusted to a concentration of 40 ± 10 mg/L Ca and 20 ± 10 mg/L Ca for oysters and belemnites, respectively. Every sample was analysed with 5 runs applying truly simultaneous acquisition times to all spectral lines investigated. Raw data in [cps] was exported and processed with external spreadsheet software combining intensity-ratio calibration after de Villiers et al. (2002) and standard-sample-standard bracketing and drift correction procedures after Schrag (1999). Data for oysters were normalized to ECRM-752 with Mg/Ca 3.821 mmol/mol and Sr/Ca 0.174 mmol/mol (Greaves et al., 2008), and data for belemnites were normalized to in-house standard sample belemnite Ja002 with Mg/Ca 16.42 Mg/Ca and Sr/Ca 0.3739 mmol/mol. Average uncertainty as estimated from 5 runs was 1.3 and 1.2 ‰ (1SD) for Mg/Ca and Sr/Ca in oysters, respectively, and 1.6 and 1.3 ‰ (1SD) in belemnites. Corals at 8 mg/L Ca typically yield uncertainties of 0.7-0.9 ‰ (1SD) for Sr/Ca. Duplicate sample analyses after approx. 90 minutes, and samples from the beginning of an analytical session re-analysed at the end of the session after ten or more hours yield average reproducibilities in the same range. Reference materials Coral JCp-1, Tridacna JCt-1, limestones ECRM 752, and CAL-S were used as secondary standards using consensus values from Hathorne et al. (2013) and Greaves et al. (2008).

Detailed description of the stable isotope record

Results of the stable isotope analyses of bivalve and brachiopod shells of northern Africa and western Asia are listed in Table S2.

Analysed shells from Morocco include a specimen of *Gryphaea* sp. from the ?Toarcian-Aalenian ($\delta^{18}O$: -2.84 ‰; $\delta^{13}C$: 3.83 ‰), one shell of *Exogyra chouberti* from the Bajocian ($\delta^{18}O$: -1.91 ‰; $\delta^{13}C$: 1.56 ‰), a rhynchonellid brachiopod from the Callovian ($\delta^{18}O$: -1.66 ‰; $\delta^{13}C$: 1.02 ‰), and one specimen of *Nanogyra nana* from the Oxfordian ($\delta^{18}O$: -1.68 ‰; $\delta^{13}C$: 2.34 ‰). Due to the scarcity of the data, no reliable trends through time can be discerned.

The collection from Tunisia includes 41 seemingly well-preserved rhynchonellid brachiopods with Early to Late Callovian ages (Fig. S3). Throughout time, $\delta^{18}O$ values vary around an overall average of -2.66 ‰ (minimum: -3.73 ‰; maximum: -1.76 ‰). Short-term fluctuations in $\delta^{18}O$ values can be seen (e.g., the most negative $\delta^{18}O$ values being reached around the Middle to Late Callovian boundary), but no long-term temporal trend can be found. The $\delta^{13}C$ values fluctuate more strongly around an overall average of 2.65 ‰ (minimum: 0.09 ‰; maximum: 4.50 ‰). From relatively high $\delta^{13}C$ values at the beginning of the Callovian (average: 3.82 ‰), values decrease to 0.53 ‰ before more or less steadily rising again towards the Late Callovian (average: 2.66 ‰).

The collection from Egypt consists of 51 well-preserved rhynchonellid brachiopods and 22 bivalves with Bajocian to Kimmeridgian ages. Their stable isotope data has been described already in detail by Alberti et al. (2017), but is presented here again with an updated lithostratigraphic correlation at higher stratigraphic resolution (Fig. S4). The results of the stable isotope analyses show relatively equable conditions through time with an overall average $\delta^{18}O$ value of -3.20 ‰ and an average $\delta^{13}C$ value of 1.50 ‰ (for more information see Alberti et al., 2017).

The stable isotope dataset of Israel includes results of 26 bivalves and 9 brachiopods with Late Bajocian, Callovian, and Early Cretaceous ages (Fig. S5). The $\delta^{18}O$ record starts with relatively low values in the Late Bajocian (average: -4.06 ‰). The $\delta^{18}O$ values are slightly higher in the Middle Callovian (Coronatum Zone, average: -3.37 ‰) and remain at similar values in the Late Callovian (Athleta Zone, average: -3.54 ‰; Lamberti Zone, average: -3.36 ‰). Four oysters from the Early Cretaceous show comparable $\delta^{18}O$ values around an average of -3.58 ‰. The $\delta^{13}C$ values show a slight increase throughout the studied time interval. Their record starts with comparatively low values in the Late Bajocian (average: 2.01 ‰). Middle Callovian (Coronatum Zone) $\delta^{13}C$ values are scattered around an average of 2.55 ‰, while Late Callovian values are still higher (Athleta Zone, average: 2.99 ‰; Lamberti Zone, average: 3.63 ‰). The Early Cretaceous oysters show $\delta^{13}C$ values around an average of 2.88 ‰.

Material from Jordan includes 22 seemingly well-preserved bivalves with Bajocian to Callovian

Table S2 Results of the stable isotope ($\delta^{18}O$, $\delta^{13}C$) analyses of samples from northern Africa and western Asia ([1]Water temperatures based on the equation of Anderson and Arthur (1983) and a $\delta^{18}O_{sea}$ value of -1 ‰, [2]$\delta^{18}O_{sea}$ value calculated for the palaeolatitude with equation (4), [3]Water temperatures based on the equation of Anderson and Arthur (1983) and a $\delta^{18}O_{sea}$ value calculated with equation (4) for the palaeolatitude).

sample no.	taxonomy	group	age	bed	locality	coordinates	palaeolatitude	$\delta^{13}C$	$\delta^{18}O$	T (°C)[1]	$\delta^{18}O_{sea}$[2]	T (°C)[3]
Morocco												
well-preserved fossils												
MO18-007	*Gryphaea* sp.	bivalve	?Toa.-Aal.	-	MO-1	31.272°. -6.072°	29.3	3.83	-2.84	24.0	-0.17	28.0
MO18-005	*Exogyra chouberti*	bivalve	Bajocian	-	MO-2	-	27.1	1.56	-1.91	19.9	-0.10	23.9
MO18-006	rhynchonellid	brachiopod	Callovian	-	MO-3	30.620°. -9.400°	27.4	1.02	-1.66	18.8	-0.11	22.7
MO18-002-A2B	*Nanogyra nana*	bivalve	Oxfordian	-	MO-4	31.208°. -9.579°	28.1	2.34	-1.68	18.9	-0.13	22.7
sediment & cement												
MO18-003Sed	-	sediment fill	Bajocian	-	MO-2	-	27.1	-0.73	-2.43	-	-	-
MO18-005Cem	-	cement fill	Bajocian	-	MO-2	-	27.1	0.33	-2.52	-	-	-
MO18-006Sed	-	sediment fill	Callovian	-	MO-3	20.620°. -9.400°	27.4	0.64	-2.51	-	-	-
poorly preserved fossils												
MO18-003	rhynchonellid	brachiopod	Bajocian	-	MO-2	-	27.1	-0.06	-3.25	-	-	-
Tunisia												
well-preserved fossils												
TU17-034-A2B	*Septirhynchia pulchra*	brachiopod	E.-M. Callovian	r2/26/4	TU-4	32.735°. 10.478°	13.7	4.50	-2.46	22.3	0.07	27.3
TU17-036	*Septirhynchia pulchra*	brachiopod	E.-M. Callovian	r2/26/4	TU-4	32.735°. 10.478°	13.7	2.95	-3.28	26.1	0.07	31.4
TU17-037	*Septirhynchia pulchra*	brachiopod	E.-M. Callovian	r2/26/4	TU-4	32.735°. 10.478°	13.7	3.99	-2.18	21.1	0.07	26.0
TU17-008	rhynchonellid	brachiopod	E.-M. Callovian	3/22/2	TU-7	33.045°. 10.380°	14.0	0.53	-2.09	20.7	0.08	25.6
TU17-039	*Septirhynchia pulchra*	brachiopod	E.-M. Callovian	p5/12/4	TU-6	32.970°. 10.450°	13.9	1.72	-2.49	22.4	0.08	27.5
TU17-040ab	*Septirhynchia pulchra*	brachiopod	E.-M. Callovian	p5/12/4	TU-6	32.970°. 10.450°	13.9	0.79	-2.80	23.9	0.08	29.0
TU17-002	*Somalirhynchia* cf. *africana*	brachiopod	E.-M. Callovian	s3/17/8	TU-1	32.250°. 10.545°	13.3	2.13	-3.09	25.2	0.07	30.4
TU17-003	*Somalirhynchia* cf. *africana*	brachiopod	E.-M. Callovian	s3/17/8	TU-1	32.250°. 10.545°	13.3	3.57	-2.93	24.5	0.07	29.6
TU17-024	rhynchonellid	brachiopod	E.-M. Callovian	s3/17/8	TU-1	32.250°. 10.545°	13.3	2.58	-3.73	28.3	0.07	33.6
TU17-001	*Somalirhynchia* cf. *africana*	brachiopod	E.-M. Callovian	r3/2/7	TU-4	32.735°. 10.478°	13.7	2.82	-2.78	23.8	0.07	28.9
TU17-019	*Somalirhynchia smelliei*	brachiopod	E.-M. Callovian	r3/2/8	TU-4	32.735°. 10.478°	13.7	3.03	-3.39	26.6	0.07	31.9
TU17-011-2AB	*Kallirhynchia africana*	brachiopod	Late Callovian	f3/6/1	TU-2	32.462°. 10.426°	13.5	2.72	-2.62	23.1	0.07	28.1
TU17-012	*Kallirhynchia africana*	brachiopod	Late Callovian	f3/6/1	TU-2	32.462°. 10.426°	13.5	2.28	-2.52	22.6	0.07	27.6
TU17-013ab	*Kallirhynchia africana*	brachiopod	Late Callovian	f3/6/1	TU-2	32.462°. 10.426°	13.5	3.10	-2.24	21.3	0.07	26.3
TU17-014ab	*Kallirhynchia africana*	brachiopod	Late Callovian	f3/6/1	TU-2	32.462°. 10.426°	13.5	3.01	-2.58	22.9	0.07	27.9
TU17-015ab	*Kallirhynchia africana*	brachiopod	Late Callovian	f3/6/1	TU-2	32.462°. 10.426°	13.5	0.09	-3.63	27.8	0.07	33.1
TU17-016	*Kallirhynchia africana*	brachiopod	Late Callovian	f3/6/1	TU-2	32.462°. 10.426°	13.5	2.87	-2.99	24.7	0.07	29.9
TU17-042ab	*Somalirhynchia smelliei*	brachiopod	Late Callovian	m5/8/4	TU-3	32.617°. 10.400°	13.7	3.40	-2.41	22.1	0.07	27.1
TU17-043	*Somalirhynchia smelliei*	brachiopod	Late Callovian	m5/8/4	TU-3	32.617°. 10.400°	13.7	2.85	-2.66	23.2	0.07	28.3
TU17-044-A2B	*Somalirhynchia smelliei*	brachiopod	Late Callovian	m5/8/4	TU-3	32.617°. 10.400°	13.7	3.31	-2.60	23.0	0.07	28.0
TU17-045-A2B	*Somalirhynchia smelliei*	brachiopod	Late Callovian	m5/8/4	TU-3	32.617°. 10.400°	13.7	3.05	-2.89	24.3	0.07	29.4
TU17-046ab	*Somalirhynchia smelliei*	brachiopod	Late Callovian	m5/8/4	TU-3	32.617°. 10.400°	13.7	3.23	-2.96	24.6	0.07	29.8
TU17-047-A2B	*Somalirhynchia smelliei*	brachiopod	Late Callovian	m5/8/4	TU-3	32.617°. 10.400°	13.7	2.87	-2.63	23.1	0.07	28.2
TU17-004ab	rhynchonellid	brachiopod	Late Callovian	gt3/24/1	TU-7	33.045°. 10.380°	14.0	4.08	-1.83	19.5	0.08	24.3
TU17-005	rhynchonellid	brachiopod	Late Callovian	gt3/24/1	TU-7	33.045°. 10.380°	14.0	3.00	-2.31	21.6	0.08	26.6
TU17-006A	rhynchonellid	brachiopod	Late Callovian	gt3/24/1	TU-7	33.045°. 10.380°	14.0	2.94	-2.22	21.2	0.08	26.2
TU17-032	*Rhynchonella tazerdunensis*	brachiopod	Late Callovian	r/3/3/1	TU-4	32.735°. 10.478°	13.7	2.83	-2.66	23.2	0.07	28.3

Table S2 (continued) Results of the stable isotope ($\delta^{18}O$, $\delta^{13}C$) analyses of samples from northern Africa and western Asia ([1]Water temperatures based on the equation of Anderson and Arthur (1983) and a $\delta^{18}O_{sea}$ value of -1 ‰, [2]$\delta^{18}O_{sea}$ value calculated for the palaeolatitude with equation (4), [3]Water temperatures based on the equation of Anderson and Arthur (1983) and a $\delta^{18}O_{sea}$ value calculated with equation (4) for the palaeolatitude).

sample no.	taxonomy	group	age	bed	locality	coordinates	palaeolatitude	$\delta^{13}C$	$\delta^{18}O$	T (°C)[1]	$\delta^{18}O_{sea}$[2]	T (°C)[3]
TU17-033ab	*Rhynchonella tazerdunensis*	brachiopod	Late Callovian	r/3/3/1	TU-4	32.735°. 10.478°	13.7	2.59	-3.03	24.9	0.07	30.1
TU17-022-AB	*Rhynchonella djeffarae*	brachiopod	Late Callovian	gt3/24/6	TU-7	33.045°. 10.380°	14.0	2.74	-1.76	19.2	0.08	24.0
TU17-023ab	*Rhynchonella djeffarae*	brachiopod	Late Callovian	gt3/24/6	TU-7	33.045°. 10.380°	14.0	1.62	-2.64	23.1	0.08	28.2
TU17-026ab	*Daghanirhynchia angulocostata*	brachiopod	Late Callovian	k5/5/2-1	TU-5	32.790°. 10.515°	13.8	0.81	-3.48	27.1	0.08	32.4
TU17-027ab	*Daghanirhynchia angulocostata*	brachiopod	Late Callovian	k5/5/2-1	TU-5	32.790°. 10.515°	13.8	1.85	-2.50	22.5	0.08	27.5
TU17-028	*Daghanirhynchia angulocostata*	brachiopod	Late Callovian	k5/5/2-1	TU-5	32.790°. 10.515°	13.8	2.39	-2.45	22.3	0.08	27.3
TU17-029	*Daghanirhynchia angulocostata*	brachiopod	Late Callovian	k5/5/2-1	TU-5	32.790°. 10.515°	13.8	1.97	-2.85	24.1	0.08	29.2
TU17-030	*Daghanirhynchia angulocostata*	brachiopod	Late Callovian	k5/5/2-1	TU-5	32.790°. 10.515°	13.8	2.42	-1.77	19.3	0.08	24.1
TU17-031	*Daghanirhynchia angulocostata*	brachiopod	Late Callovian	k5/5/2-1	TU-5	32.790°. 10.515°	13.8	1.96	-2.78	23.8	0.08	28.9
TU17-017A	*Somalirhynchia* cf. *africana*	brachiopod	Late Callovian	r3/3/5	TU-4	32.735°. 10.478°	13.7	2.83	-2.51	22.5	0.07	27.6
TU17-018ab	*Somalirhynchia* cf. *africana*	brachiopod	Late Callovian	r3/3/5	TU-4	32.735°. 10.478°	13.7	4.18	-2.19	21.1	0.07	26.1
TU17-009	*Somalirhynchia* cf. *africana*	brachiopod	Late Callovian	f3/9/2	TU-2	32.462°. 10.426°	13.5	3.15	-2.80	23.9	0.07	29.0
TU17-010ab	*Somalirhynchia* cf. *africana*	brachiopod	Late Callovian	f3/9/2	TU-2	32.462°. 10.426°	13.5	2.83	-2.77	23.7	0.07	28.8
TU17-038-AB	*Somalirhynchia smelliei*	brachiopod	Late Callovian	m5/9/21	TU-3	32.617°. 10.400°	13.7	2.95	-2.71	23.5	0.07	28.5
sediment & cement												
TU17-045C	-	cement	Late Callovian	m5/8/4	TU-3	32.617°. 10.400°	13.7	1.09	-7.14	-	-	-
TU17-045D	-	sediment fill	Late Callovian	m5/8/4	TU-3	32.617°. 10.400°	13.7	0.54	-2.39	-	-	-
TU17-006B	-	cement	Late Callovian	gt3/24/1	TU-7	33.045°. 10.380°	14.0	1.00	-6.03	-	-	-
TU17-021B	-	cement	Late Callovian	gt3/24/6	TU-7	33.045°. 10.380°	14.0	1.34	-11.88	-	-	-
TU17-017B	-	sediment fill	Late Callovian	r3/3/5	TU-4	32.735°. 10.478°	13.7	0.45	-2.56	-	-	-
poorly preserved fossils												
TU17-035	*Septirhynchia pulchra*	brachiopod	E.-M. Callovian	r2/26/4	TU-4	32.735°. 10.478°	13.7	-1.42	-3.91	-	-	-
TU17-041A	*Septirhynchia pulchra*	brachiopod	E.-M. Callovian	p5/12/4	TU-6	32.970°. 10.450°	13.9	0.54	-3.96	-	-	-
TU17-041B	*Septirhynchia pulchra*	brachiopod	E.-M. Callovian	p5/12/4	TU-6	32.970°. 10.450°	13.9	-0.42	-4.78	-	-	-
Egypt												
well-preserved fossils												
H1-1	*Cymatorhynchia quadriplicata*	brachiopod	Early Bajocian	H1	EG-1	30.647°. 33.328°	3.3	1.63	-3.17	25.6	-0.16	29.6
M1-1	*Cymatorhynchia quadriplicata*	brachiopod	Early Bajocian	M1	EG-4	30.682°. 33.422°	3.3	1.67	-3.37	26.6	-0.16	30.7
A5-1	*Africogryphaea costellata*	bivalve	Late Bajocian	A5	EG-2	30.677°. 33.355°	3.3	2.43	-3.42	26.8	-0.16	30.9
A6-1	*Daghanirhynchia daghaniensis*	brachiopod	Late Bajocian	A6	EG-2	30.677°. 33.355°	3.3	1.61	-3.05	25.0	-0.16	29.0
A6-2	*Daghanirhynchia daghaniensis*	brachiopod	Late Bajocian	A6	EG-2	30.677°. 33.355°	3.3	1.75	-2.86	24.2	-0.16	28.1
A7-2	*Conarosia rotundata*	brachiopod	Late Bajocian	A7	EG-2	30.677°. 33.355°	3.3	1.28	-3.14	25.5	-0.16	29.5
A9-1	*Conarosia rotundata*	brachiopod	Late Bajocian	A9	EG-2	30.677°. 33.355°	3.3	1.14	-2.49	22.5	-0.16	26.4
A9-2	*Conarosia rotundata*	brachiopod	Late Bajocian	A9	EG-2	30.677°. 33.355°	3.3	1.57	-3.35	26.4	-0.16	30.5
H3-1	*Daghanirhynchia angulocostata*	brachiopod	Early Bathonian	H3	EG-1	30.647°. 33.328°	3.3	1.38	-3.36	26.5	-0.16	30.6
H3-3	*Daghanirhynchia angulocostata*	brachiopod	Early Bathonian	H3	EG-1	30.647°. 33.328°	3.3	0.73	-3.62	27.7	-0.16	31.9
A10-1	*Conarosia rotundata*	brachiopod	Early Bathonian	A10	EG-2	30.677°. 33.355°	3.3	2.71	-3.02	24.9	-0.16	28.9
A11-1	*Cymatorhynchia quadriplicata*	brachiopod	Early Bathonian	A11	EG-2	30.677°. 33.355°	3.3	1.34	-3.90	29.1	-0.16	33.3
H6-1	*Daghanirhynchia daghaniensis*	brachiopod	Middle Bathonian	H6	EG-1	30.647°. 33.328°	3.3	1.30	-3.06	25.1	-0.16	29.1
H6-2	*Daghanirhynchia daghaniensis*	brachiopod	Middle Bathonian	H6	EG-1	30.647°. 33.328°	3.3	1.60	-2.77	23.8	-0.16	27.7
H6-3	*Daghanirhynchia daghaniensis*	brachiopod	Middle Bathonian	H6	EG-1	30.647°. 33.328°	3.3	1.79	-3.19	25.7	-0.16	29.8

Table S2 (continued) Results of the stable isotope ($\delta^{18}O$, $\delta^{13}C$) analyses of samples from northern Africa and western Asia ([1]Water temperatures based on the equation of Anderson and Arthur (1983) and a $\delta^{18}O_{sea}$ value of -1 ‰, [2]$\delta^{18}O_{sea}$ value calculated for the palaeolatitude with equation (4), [3]Water temperatures based on the equation of Anderson and Arthur (1983) and a $\delta^{18}O_{sea}$ value calculated with equation (4) for the palaeolatitude).

sample no.	taxonomy	group	age	bed	locality	coordinates	palaeolatitude	$\delta^{13}C$	$\delta^{18}O$	T (°C)[1]	$\delta^{18}O_{sea}$[2]	T (°C)[3]
A13-1	*Daghanirhynchia daghaniensis*	brachiopod	Middle Bathonian	A13	EG-2	30.677°. 33.355°	3.3	1.32	-3.38	26.6	-0.16	30.7
A14-1	*Daghanirhynchia angulocostata*	brachiopod	Middle Bathonian	A14	EG-2	30.677°. 33.355°	3.3	1.78	-3.29	26.2	-0.16	30.3
A14-2-ab	*Daghanirhynchia angulocostata*	brachiopod	Middle Bathonian	A14	EG-2	30.677°. 33.355°	3.3	0.94	-3.87	28.9	-0.16	33.1
A14-3	*Daghanirhynchia angulocostata*	brachiopod	Middle Bathonian	A14	EG-2	30.677°. 33.355°	3.3	1.99	-3.24	25.9	-0.16	30.0
A14-4	*Daghanirhynchia angulocostata*	brachiopod	Middle Bathonian	A14	EG-2	30.677°. 33.355°	3.3	1.70	-3.17	25.6	-0.16	29.7
A15-1	*Daghanirhynchia daghaniensis*	brachiopod	Middle Bathonian	A15	EG-2	30.677°. 33.355°	3.3	1.19	-3.59	27.6	-0.16	31.8
H8-3	*Daghanirhynchia daghaniensis*	brachiopod	Middle Bathonian	H8	EG-1	30.647°. 33.328°	3.3	1.01	-3.17	25.6	-0.16	29.7
A17-1	*Burmirhynchia cavagnarii*	brachiopod	Middle Bathonian	A17	EG-2	30.677°. 33.355°	3.3	1.36	-3.01	24.9	-0.16	28.9
A17-2	*Burmirhynchia cavagnarii*	brachiopod	Middle Bathonian	A17	EG-2	30.677°. 33.355°	3.3	0.33	-3.43	26.8	-0.16	30.9
A17-3	*Burmirhynchia cavagnarii*	brachiopod	Middle Bathonian	A17	EG-2	30.677°. 33.355°	3.3	1.28	-3.28	26.1	-0.16	30.2
E7-1-ab	*Africogryphaea costellata*	bivalve	Middle Bathonian	E7	EG-3	30.698°. 33.387°	3.3	1.33	-3.72	28.2	-0.16	32.4
E7-2	*Africogryphaea costellata*	bivalve	Middle Bathonian	E7	EG-3	30.698°. 33.387°	3.3	1.41	-3.81	28.6	-0.16	32.8
E7-3	*Africogryphaea costellata*	bivalve	Middle Bathonian	E7	EG-3	30.698°. 33.387°	3.3	1.67	-3.54	27.3	-0.16	31.5
M11-1	*Africogryphaea costellata*	bivalve	Middle Bathonian	M11	EG-4	30.682°. 33.422°	3.3	1.34	-3.22	25.9	-0.16	29.9
M11-2	*Africogryphaea costellata*	bivalve	Middle Bathonian	M11	EG-4	30.682°. 33.422°	3.3	1.36	-3.19	25.7	-0.16	29.7
M11-3	*Africogryphaea costellata*	bivalve	Middle Bathonian	M11	EG-4	30.682°. 33.422°	3.3	0.48	-2.91	24.4	-0.16	28.4
M11-4-ab	*Daghanirhynchia daghaniensis*	brachiopod	Middle Bathonian	M11	EG-4	30.682°. 33.422°	3.3	0.56	-2.95	24.6	-0.16	28.6
M11-5	*Daghanirhynchia daghaniensis*	brachiopod	Middle Bathonian	M11	EG-4	30.682°. 33.422°	3.3	1.02	-2.85	24.1	-0.16	28.1
M11-6	*Daghanirhynchia daghaniensis*	brachiopod	Middle Bathonian	M11	EG-4	30.682°. 33.422°	3.3	0.50	-3.11	25.3	-0.16	29.3
E9-1	*Daghanirhynchia angulocostata*	brachiopod	Middle Bathonian	E9	EG-3	30.698°. 33.387°	3.3	1.27	-3.14	25.5	-0.16	29.5
E9-2	*Daghanirhynchia angulocostata*	brachiopod	Middle Bathonian	E9	EG-3	30.698°. 33.387°	3.3	1.43	-2.93	24.5	-0.16	28.5
E9-3	*Daghanirhynchia angulocostata*	brachiopod	Middle Bathonian	E9	EG-3	30.698°. 33.387°	3.3	1.37	-2.99	24.8	-0.16	28.8
E9-4	*Daghanirhynchia angulocostata*	brachiopod	Middle Bathonian	E9	EG-3	30.698°. 33.387°	3.3	1.15	-3.01	24.8	-0.16	28.8
H9-1	*Africogryphaea costellata*	bivalve	Middle Bathonian	H9	EG-1	30.647°. 33.328°	3.3	1.43	-3.10	25.3	-0.16	29.3
H9-2	*Africogryphaea costellata*	bivalve	Middle Bathonian	H9	EG-1	30.647°. 33.328°	3.3	1.91	-2.90	24.3	-0.16	28.3
H9-3	*Africogryphaea costellata*	bivalve	Middle Bathonian	H9	EG-1	30.647°. 33.328°	3.3	1.91	-3.15	25.5	-0.16	29.6
H9-4	*Daghanirhynchia angulocostata*	brachiopod	Middle Bathonian	H9	EG-1	30.647°. 33.328°	3.3	1.34	-3.31	26.3	-0.16	30.4
H9-5	*Daghanirhynchia angulocostata*	brachiopod	Middle Bathonian	H9	EG-1	30.647°. 33.328°	3.3	1.50	-4.01	29.6	-0.16	33.9
H9-6	*Daghanirhynchia angulocostata*	brachiopod	Middle Bathonian	H9	EG-1	30.647°. 33.328°	3.3	2.02	-3.08	25.2	-0.16	29.2
H10-2	*Daghanirhynchia daghaniensis*	brachiopod	Middle Bathonian	H10	EG-1	30.647°. 33.328°	3.3	2.08	-2.86	24.2	-0.16	28.2
H11-1	*Africogryphaea costellata*	bivalve	Middle Bathonian	H11	EG-1	30.647°. 33.328°	3.3	2.26	-2.85	24.1	-0.16	28.1
H11-2	*Africogryphaea costellata*	bivalve	Middle Bathonian	H11	EG-1	30.647°. 33.328°	3.3	1.86	-2.89	24.3	-0.16	28.3
H11-3	*Africogryphaea costellata*	bivalve	Middle Bathonian	H11	EG-1	30.647°. 33.328°	3.3	2.32	-3.06	25.1	-0.16	29.1
H11-4	*Africogryphaea costellata*	bivalve	Middle Bathonian	H11	EG-1	30.647°. 33.328°	3.3	1.53	-2.85	24.1	-0.16	28.1
H11-5	*Daghanirhynchia daghaniensis*	brachiopod	Middle Bathonian	H11	EG-1	30.647°. 33.328°	3.3	0.85	-3.63	27.8	-0.16	32.0
H11-7	*Daghanirhynchia daghaniensis*	brachiopod	Middle Bathonian	H11	EG-1	30.647°. 33.328°	3.3	2.61	-3.39	26.6	-0.16	30.7
E13-1	*Burmirhynchia cavagnarii*	brachiopod	Late Bathonian	E13	EG-3	30.698°. 33.387°	3.3	1.13	-2.79	23.8	-0.16	27.8
E13-2	*Burmirhynchia cavagnarii*	brachiopod	Late Bathonian	E13	EG-3	30.698°. 33.387°	3.3	1.40	-3.26	26.0	-0.16	30.1
E13-3	*Burmirhynchia cavagnarii*	brachiopod	Late Bathonian	E13	EG-3	30.698°. 33.387°	3.3	1.41	-3.29	26.2	-0.16	30.2
E14-1	*Africogryphaea costellata*	bivalve	Late Bathonian	E14	EG-3	30.698°. 33.387°	3.3	1.79	-3.36	26.5	-0.16	30.6
M15-1	*Africogryphaea costellata*	bivalve	Early Callovian	M15	EG-4	30.682°. 33.422°	3.4	2.21	-3.47	27.0	-0.15	31.2
M15-2	*Africogryphaea costellata*	bivalve	Early Callovian	M15	EG-4	30.682°. 33.422°	3.4	1.87	-2.75	23.6	-0.15	27.6
M16-2-ab	*Daghanirhynchia angulocostata*	brachiopod	Early Callovian	M16	EG-4	30.682°. 33.422°	3.4	1.57	-3.13	25.4	-0.15	29.5
E16-1	*Daghanirhynchia angulocostata*	brachiopod	Middle Callovian	E16	EG-3	30.698°. 33.387°	3.4	1.56	-3.26	26.0	-0.15	30.1

Table S2 (continued) Results of the stable isotope ($\delta^{18}O$, $\delta^{13}C$) analyses of samples from northern Africa and western Asia ([1]Water temperatures based on the equation of Anderson and Arthur (1983) and a $\delta^{18}O_{sea}$ value of -1 ‰, [2]$\delta^{18}O_{sea}$ value calculated for the palaeolatitude with equation (4), [3]Water temperatures based on the equation of Anderson and Arthur (1983) and a $\delta^{18}O_{sea}$ value calculated with equation (4) for the palaeolatitude).

sample no.	taxonomy	group	age	bed	locality	coordinates	palaeolatitude	$\delta^{13}C$	$\delta^{18}O$	T (°C)[1]	$\delta^{18}O_{sea}$[2]	T (°C)[3]
M20-1	*Africogryphaea costellata*	bivalve	Middle Callovian	M20	EG-4	30.682°. 33.422°	3.4	1.78	-3.35	26.5	-0.15	30.6
E18-1	*Burmirhynchia cavagnarii*	brachiopod	Late Callovian	E18	EG-3	30.698°. 33.387°	3.4	1.32	-3.32	26.3	-0.15	30.4
E18-2	*Burmirhynchia cavagnarii*	brachiopod	Late Callovian	E18	EG-3	30.698°. 33.387°	3.4	1.47	-3.66	27.9	-0.15	32.1
E18-3	Burmirhynchia cavagnarii	brachiopod	Late Callovian	E18	EG-3	30.698°. 33.387°	3.4	1.39	-3.31	26.3	-0.15	30.4
H16-1	*Daghanirhynchia angulocostata*	brachiopod	Late Callovian	H16	EG-1	30.647°. 33.328°	3.4	0.80	-3.17	25.6	-0.15	29.7
H16-2	*Daghanirhynchia angulocostata*	brachiopod	Late Callovian	H16	EG-1	30.647°. 33.328°	3.4	1.66	-3.47	27.0	-0.15	31.2
H16-3	*Daghanirhynchia angulocostata*	brachiopod	Late Callovian	H16	EG-1	30.647°. 33.328°	3.4	1.29	-3.48	27.0	-0.15	31.2
H16-5	*Nanogyra nana*	bivalve	Late Callovian	H16	EG-1	30.647°. 33.328°	3.4	1.97	-3.24	25.9	-0.15	30.0
H16-6	*Nanogyra nana*	bivalve	Late Callovian	H16	EG-1	30.647°. 33.328°	3.4	2.32	-2.90	24.3	-0.15	28.3
E22-1	*Daghanirhynchia angulocostata*	brachiopod	E. Kimmeridgian	E22	EG-3	30.698°. 33.387°	2.8	1.48	-3.17	25.6	-0.18	29.6
E22-2	*Daghanirhynchia angulocostata*	brachiopod	E. Kimmeridgian	E22	EG-3	30.698°. 33.387°	2.8	1.22	-2.96	24.6	-0.18	28.5
E22-3	*Daghanirhynchia angulocostata*	brachiopod	E. Kimmeridgian	E22	EG-3	30.698°. 33.387°	2.8	1.49	-3.12	25.4	-0.18	29.3
E22-4	*Nanogyra nana*	bivalve	E. Kimmeridgian	E22	EG-3	30.698°. 33.387°	2.8	1.43	-2.16	21.0	-0.18	24.7
E22-5	*Gryphaeligmus jabbokensis*	bivalve	E. Kimmeridgian	E22	EG-3	30.698°. 33.387°	2.8	1.74	-3.04	25.0	-0.18	28.9
sediment & cement												
A7-2S	-	sediment fill	Late Bajocian	A7	EG-2	30.677°. 33.355°	3.3	-0.90	-5.82	-	-	-
H6-3S	-	sediment fill	Middle Bathonian	H6	EG-1	30.647°. 33.328°	3.3	0.12	-2.76	-	-	-
A14-3C	-	cement fill	Middle Bathonian	A14	EG-2	30.677°. 33.355°	3.3	1.23	-8.22	-	-	-
M11-1S	-	sediment fill	Middle Bathonian	M11	EG-4	30.682°. 33.422°	3.3	-0.53	-6.38	-	-	-
M11-4S	-	sediment fill	Middle Bathonian	M11	EG-4	30.682°. 33.422°	3.3	-1.12	-6.51	-	-	-
E9-2C	-	cement fill	Middle Bathonian	E19	EG-3	30.698°. 33.387°	3.3	0.61	-6.19	-	-	-
E13-1C	-	cement fill	Late Bathonian	E13	EG-3	30.698°. 33.387°	3.3	0.48	-6.72	-	-	-
H16-1C	-	cement fill	Late Callovian	H16	EG-1	30.647°. 33.328°	3.4	1.15	-9.80	-	-	-
E22-3C	-	cement fill	E. Kimmeridgian	E22	EG-3	30.698°. 33.387°	2.8	0.82	-8.09	-	-	-
poorly preserved fossils												
H10-1D	*Africogryphaea costellata*	bivalve	Middle Bathonian	H10	EG-1	30.647°. 33.328°	3.3	0.08	-5.58	-	-	-
Israel												
well-preserved fossils												
IS17-060	rhynchonellid	brachiopod	Late Bajocian	ram-5a	IS-8	30.627°. 34.842°	2.7	2.88	-4.03	29.8	-0.18	33.9
IS17-061	oyster	bivalve	Late Bajocian	ram-5a	IS-9	30.617°. 34.836°	2.7	1.14	-4.09	30.0	-0.18	34.1
IS17-035	*Somalirhynchia africana*	brachiopod	Middle Callovian	gad-11	IS-1	30.948°. 35.000°	3.0	1.01	-3.84	28.8	-0.17	33.0
IS17-036	*Eligmus* sp.	bivalve	Middle Callovian	gad-11	IS-1	30.948°. 35.000°	3.0	2.92	-2.81	23.9	-0.17	27.8
IS17-037	oyster	bivalve	Middle Callovian	gad-11	IS-1	30.948°. 35.000°	3.0	2.17	-3.46	27.0	-0.17	31.0
IS17-038	oyster	bivalve	Middle Callovian	gad-11	IS-1	30.948°. 35.000°	3.0	2.73	-3.39	26.6	-0.17	30.7
IS17-039	*Nanogyra* sp.	bivalve	Middle Callovian	gad-11	IS-1	30.948°. 35.000°	3.0	3.10	-3.34	26.4	-0.17	30.4
IS17-040	*Nanogyra* sp.	bivalve	Middle Callovian	gad-11	IS-1	30.948°. 35.000°	3.0	2.96	-3.20	25.7	-0.17	29.7
IS17-041-2A	*Nanogyra* sp.	bivalve	Middle Callovian	gad-11	IS-1	30.948°. 35.000°	3.0	3.09	-3.53	27.3	-0.17	31.4
IS17-042	*Ostrea dubiensis*	bivalve	Middle Callovian	gad-11	IS-1	30.948°. 35.000°	3.0	3.10	-3.26	26.0	-0.17	30.0
IS17-044	rhynchonellid	brachiopod	Middle Callovian	gad-11	IS-1	30.948°. 35.000°	3.0	2.18	-3.47	27.0	-0.17	31.1
IS17-045	oyster	bivalve	Middle Callovian	gad-11	IS-1	30.948°. 35.000°	3.0	2.27	-3.40	26.7	-0.17	30.7
IS17-001-AB	*Burmirhynchia jirbaensis*	brachiopod	Late Callovian	gad-43	IS-2	30.941°. 34.983°	3.0	2.38	-3.91	29.2	-0.17	33.3

Table S2 (continued) Results of the stable isotope ($\delta^{18}O$, $\delta^{13}C$) analyses of samples from northern Africa and western Asia ([1]Water temperatures based on the equation of Anderson and Arthur (1983) and a $\delta^{18}O_{sea}$ value of -1 ‰, [2]$\delta^{18}O_{sea}$ value calculated for the palaeolatitude with equation (4), [3]Water temperatures based on the equation of Anderson and Arthur (1983) and a $\delta^{18}O_{sea}$ value calculated with equation (4) for the palaeolatitude).

sample no.	taxonomy	group	age	bed	locality	coordinates	palaeolatitude	δ13C	δ18O	T (°C)[1]	$\delta^{18}O_{sea}$[2]	T (°C)[3]
IS17-004	*Gryphaea* sp.	bivalve	Late Callovian	gad-43	IS-2	30.941°. 34.983°	3.0	3.18	-3.58	27.5	-0.17	31.6
IS17-005	rhynchonellid	brachiopod	Late Callovian	gad-43	IS-2	30.941°. 34.983°	3.0	1.93	-3.27	26.1	-0.17	30.1
IS17-006	rhynchonellid	brachiopod	Late Callovian	gad-43	IS-2	30.941°. 34.983°	3.0	1.65	-4.34	31.3	-0.17	35.5
IS17-008	*Nanogyra* sp.	bivalve	Late Callovian	gad-43	IS-2	30.941°. 34.983°	3.0	3.16	-3.67	28.0	-0.17	32.1
IS17-009	*Somalirhynchia africana*	brachiopod	Late Callovian	gad-43	IS-2	30.941°. 34.983°	3.0	2.59	-4.20	30.6	-0.17	34.8
IS17-012	*Nanogyra* sp.	bivalve	Late Callovian	gad-43	IS-2	30.941°. 34.983°	3.0	3.44	-3.23	25.9	-0.17	29.9
IS17-020	*Actinostreon* sp.	bivalve	Late Callovian	gad-47	IS-3	30.941°. 34.982°	3.0	3.36	-3.86	28.9	-0.17	33.1
IS17-055	*Ostrea* sp.	bivalve	Late Callovian	gad-48	IS-4	30.941°. 34.981°	3.0	3.95	-2.97	24.7	-0.17	28.6
IS17-057	*Ostrea* sp.	bivalve	Late Callovian	gad-48	IS-4	30.941°. 34.981°	3.0	3.76	-3.29	26.2	-0.17	30.2
IS17-058	*Nanogyra* sp.	bivalve	Late Callovian	gad-48	IS-4	30.941°. 34.981°	3.0	3.49	-2.64	23.2	-0.17	27.0
IS17-046	*Burmirhynchia jirbaensis*	brachiopod	Late Callovian	gad-60/61	IS-5	30.942°. 34.980°	3.0	3.72	-3.07	25.1	-0.17	29.1
IS17-059	oyster	bivalve	Late Callovian	gad-62	IS-6	30.943°. 34.980°	3.0	2.68	-3.58	27.5	-0.17	31.6
IS17-023-AB	oyster	bivalve	Late Callovian	gad-63	IS-7	30.943°. 34.980°	3.0	3.49	-3.30	26.2	-0.17	30.2
IS17-025	*Nanogyra* sp.	bivalve	Late Callovian	gad-63	IS-7	30.943°. 34.980°	3.0	3.93	-3.56	27.4	-0.17	31.5
IS17-026	*Nanogyra* sp.	bivalve	Late Callovian	gad-63	IS-7	30.943°. 34.980°	3.0	4.71	-3.31	26.3	-0.17	30.3
IS17-028-AB	*Actinostreon* sp.	bivalve	Late Callovian	gad-63	IS-7	30.943°. 34.980°	3.0	4.28	-3.27	26.0	-0.17	30.1
IS17-029	*Nanogyra* sp.	bivalve	Late Callovian	gad-63	IS-7	30.943°. 34.980°	3.0	3.88	-3.20	25.7	-0.17	29.7
IS17-032	rhynchonellid	brachiopod	Late Callovian	gad-63	IS-7	30.943°. 34.980°	3.0	2.35	-3.59	27.6	-0.17	31.7
IS17-066	*Exogyra* sp.	bivalve	Early Cretaceous	ram-Cr	IS-10	30.624°. 34.842°	2.0	2.81	-3.14	25.5	-0.22	29.2
IS17-067	*Exogyra* sp.	bivalve	Early Cretaceous	ram-Cr	IS-10	30.624°. 34.842°	2.0	2.73	-3.36	26.5	-0.22	30.3
IS17-068	*Exogyra* sp.	bivalve	Early Cretaceous	ram-Cr	IS-10	30.624°. 34.842°	2.0	3.27	-3.91	29.2	-0.22	33.1
IS17-069	*Exogyra* sp.	bivalve	Early Cretaceous	ram-Cr	IS-10	30.624°. 34.842°	2.0	2.72	-3.90	29.1	-0.22	33.0
sediment & cement												
IS17-035Sed	-	sediment fill	Middle Callovian	gad-11	IS-1	30.948°. 35.000°	3.0	2.11	-4.51	-	-	-
IS17-003Sed	-	sediment fill	Late Callovian	gad-43	IS-2	30.941°. 34.983°	3.0	1.86	-3.81	-	-	-
IS17-013Cem	-	cement fill	Late Callovian	gad-47	IS-3	30.941°. 34.982°	3.0	2.29	-6.74	-	-	-
IS17-014Cem	-	cement fill	Late Callovian	gad-47	IS-3	30.941°. 34.982°	3.0	1.86	-7.84	-	-	-
IS17-036Sed	-	sediment fill	Middle Callovian	gad-11	IS-1	30.948°. 35.000°	3.0	2.01	-3.45	-	-	-
Jordan												
well-preserved fossils												
JO18-028	*Africogryphaea costellata*	bivalve	Bajocian	a-10	JO-2	32.125°. 35.654°	1.7	2.15	-2.55	22.7	-0.23	26.3
JO18-029	*Africogryphaea costellata*	bivalve	Bajocian	a-10	JO-2	32.125°. 35.654°	1.7	2.22	-3.04	25.0	-0.23	28.7
JO18-033	*Africogryphaea costellata*	bivalve	Bathonian	h-6	JO-3	32.175°. 35.705°	1.8	2.13	-2.69	23.4	-0.23	27.0
JO18-034	*Africogryphaea costellata*	bivalve	Bathonian	h-6	JO-3	32.175°. 35.705°	1.8	2.33	-2.63	23.1	-0.23	26.7
JO18-024	*Africogryphaea costellata*	bivalve	Bathonian	r-1	JO-1	32.108°. 35.660°	1.7	1.80	-2.44	22.2	-0.23	25.8
JO18-025	*Africogryphaea costellata*	bivalve	Bathonian	r-1	JO-1	32.108°. 35.660°	1.7	2.14	-2.78	23.8	-0.23	27.4
JO18-027	*Africogryphaea costellata*	bivalve	Bathonian	r-1	JO-1	32.108°. 35.660°	1.7	1.65	-3.54	27.4	-0.23	31.1
JO18-030	*Gryphaeligmus jabbokensis*	bivalve	Bathonian	r-1	JO-1	32.108°. 35.660°	1.7	2.08	-3.67	28.0	-0.23	31.8
JO18-031	*Gryphaeligmus jabbokensis*	bivalve	Bathonian	r-1	JO-1	32.108°. 35.660°	1.7	1.58	-3.07	25.1	-0.23	28.8
JO18-032	*Gryphaeligmus jabbokensis*	bivalve	Bathonian	r-1	JO-1	32.108°. 35.660°	1.7	2.22	-3.48	27.1	-0.23	30.8
JO18-035	*Eligmus rollandi*	bivalve	Bathonian	r-1	JO-1	32.108°. 35.660°	1.7	1.95	-3.47	27.0	-0.23	30.8
JO18-036	*Eligmus rollandi*	bivalve	Bathonian	r-1	JO-1	32.108°. 35.660°	1.7	1.59	-3.12	25.4	-0.23	29.1

Table S2 (continued) Results of the stable isotope ($\delta^{18}O$, $\delta^{13}C$) analyses of samples from northern Africa and western Asia ([1]Water temperatures based on the equation of Anderson and Arthur (1983) and a $\delta^{18}O_{sea}$ value of -1 ‰, [2]$\delta^{18}O_{sea}$ value calculated for the palaeolatitude with equation (4), [3]Water temperatures based on the equation of Anderson and Arthur (1983) and a $\delta^{18}O_{sea}$ value calculated with equation (4) for the palaeolatitude).

sample no.	taxonomy	group	age	bed	locality	coordinates	palaeolatitude	$\delta^{13}C$	$\delta^{18}O$	T (°C)[1]	$\delta^{18}O_{sea}$ [2]	T (°C)[3]
JO18-003	*Gryphaeligmus jabbokensis*	bivalve	Bathonian	s-2	JO-4	32.189°. 35.713°	1.8	1.33	-2.88	24.3	-0.23	27.9
JO18-004	*Gryphaeligmus jabbokensis*	bivalve	Bathonian	s-2	JO-4	32.189°. 35.713°	1.8	1.21	-3.08	25.2	-0.23	28.9
JO18-005	*Gryphaeligmus jabbokensis*	bivalve	Bathonian	s-2	JO-4	32.189°. 35.713°	1.8	2.17	-3.50	27.2	-0.23	31.0
JO18-016	*Africogryphaea costellata*	bivalve	Bathonian	s-h	JO-4	32.189°. 35.713°	1.8	1.69	-3.06	25.1	-0.23	28.8
JO18-018	*Africogryphaea costellata*	bivalve	Bathonian	s-h	JO-4	32.189°. 35.713°	1.8	2.06	-2.98	24.7	-0.23	28.4
JO18-023	*Africogryphaea costellata*	bivalve	Bathonian	s-h	JO-4	32.189°. 35.713°	1.8	2.10	-2.45	22.3	-0.23	25.8
JO18-019	*Gryphaeligmus jabbokensis*	bivalve	Bathonian	s-4	JO-4	32.189°. 35.713°	1.8	1.99	-4.34	31.3	-0.23	35.2
JO18-013	*Gryphaeligmus jabbokensis*	bivalve	Callovian	t-1	JO-5	32.191°. 35.800°	1.8	1.78	-4.00	29.6	-0.23	33.5
JO18-007	*Gryphaeligmus jabbokensis*	bivalve	Callovian	t-5	JO-5	32.191°. 35.800°	1.8	1.83	-4.10	30.1	-0.23	34.0
JO18-001	*Eligmus asiaticus*	bivalve	Callovian	r-11	JO-1	32.108°. 35.660°	1.8	2.13	-3.99	29.5	-0.23	33.4
sediment & cement												
JO18-003Sed	-	sediment fill	Bathonian	s-2	JO-4	32.189°. 35.713°	1.8	-0.09	-3.07	-	-	-
JO18-016Sed	-	sediment fill	Bathonian	s-h	JO-4	32.189°. 35.713°	1.8	-0.34	-5.15	-	-	-
poorly preserved fossils												
JO18-020	*Eligmus rollandi*	bivalve	Bathonian	h-6	JO-3	32.175°. 35.705°	1.8	2.35	-2.39	-	-	-
JO18-006	*Gryphaeligmus jabbokensis*	bivalve	Bathonian	s-2	JO-4	32.189°. 35.713°	1.8	1.66	-3.19	-	-	-
JO18-015	*Africogryphaea costellata*	bivalve	Bathonian	s-h	JO-4	32.189°. 35.713°	1.8	1.08	-3.28	-	-	-
JO18-021	*Africogryphaea costellata*	bivalve	Bathonian	s-h	JO-4	32.189°. 35.713°	1.8	0.95	-3.51	-	-	-
JO18-012	*Gryphaeligmus jabbokensis*	bivalve	Callovian	t-1	JO-5	32.191°. 35.800°	1.8	1.67	-3.58	-	-	-
JO18-014	*Gryphaeligmus jabbokensis*	bivalve	Callovian	t-1	JO-5	32.191°. 35.800°	1.8	1.36	-4.19	-	-	-
JO18-008	*Gryphaeligmus jabbokensis*	bivalve	Callovian	t-5	JO-5	32.191°. 35.800°	1.8	1.32	-3.38	-	-	-
JO18-009	*Gryphaeligmus jabbokensis*	bivalve	Callovian	t-5	JO-5	32.191°. 35.800°	1.8	1.07	-3.36	-	-	-

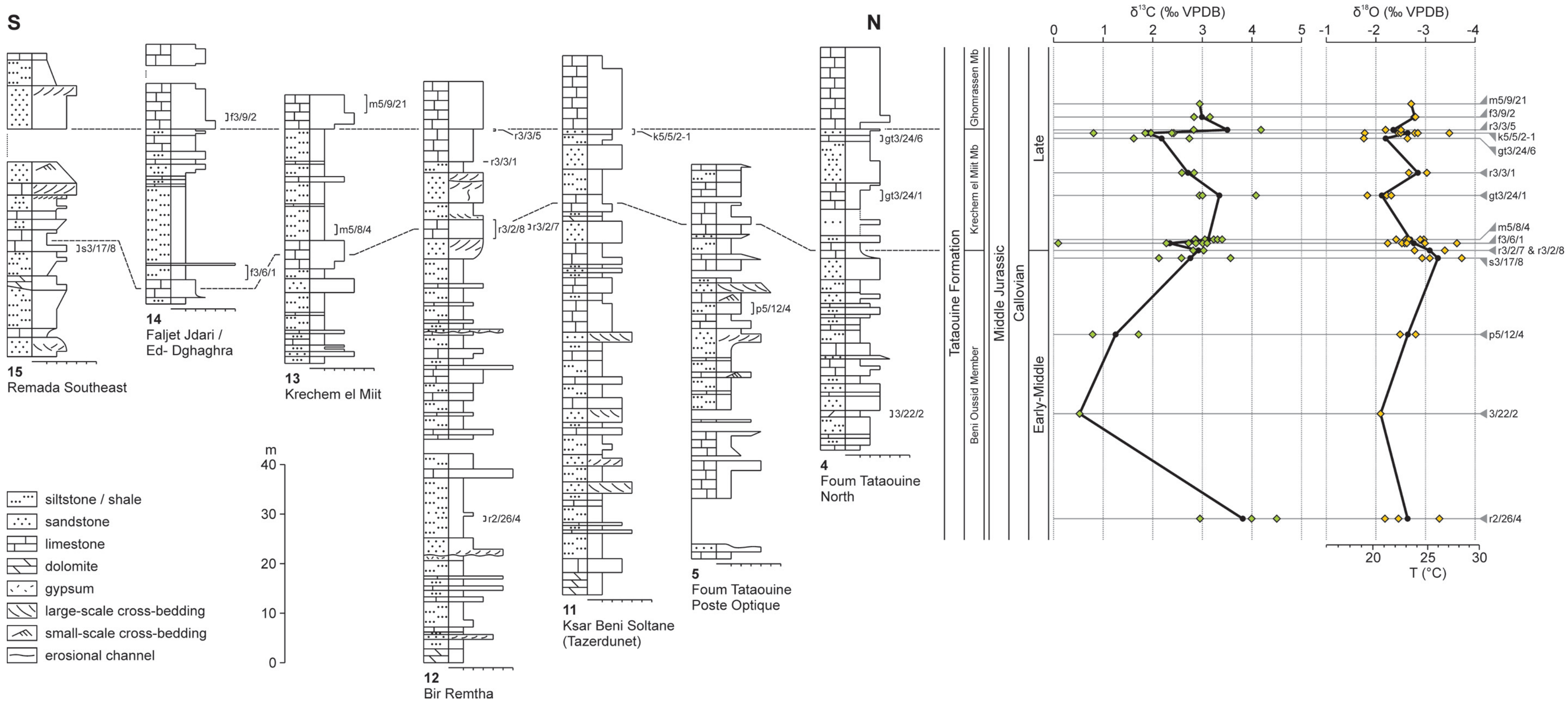

Fig. S3 Results of stable isotope ($\delta^{18}O$, $\delta^{13}C$) analyses of Callovian brachiopod shells from Tunisia (sections modified after Holzapfel, 1998). Scale for water temperatures is based on the equation of Anderson and Arthur (1983) and a $\delta^{18}O_{sea}$ value of -1 ‰.

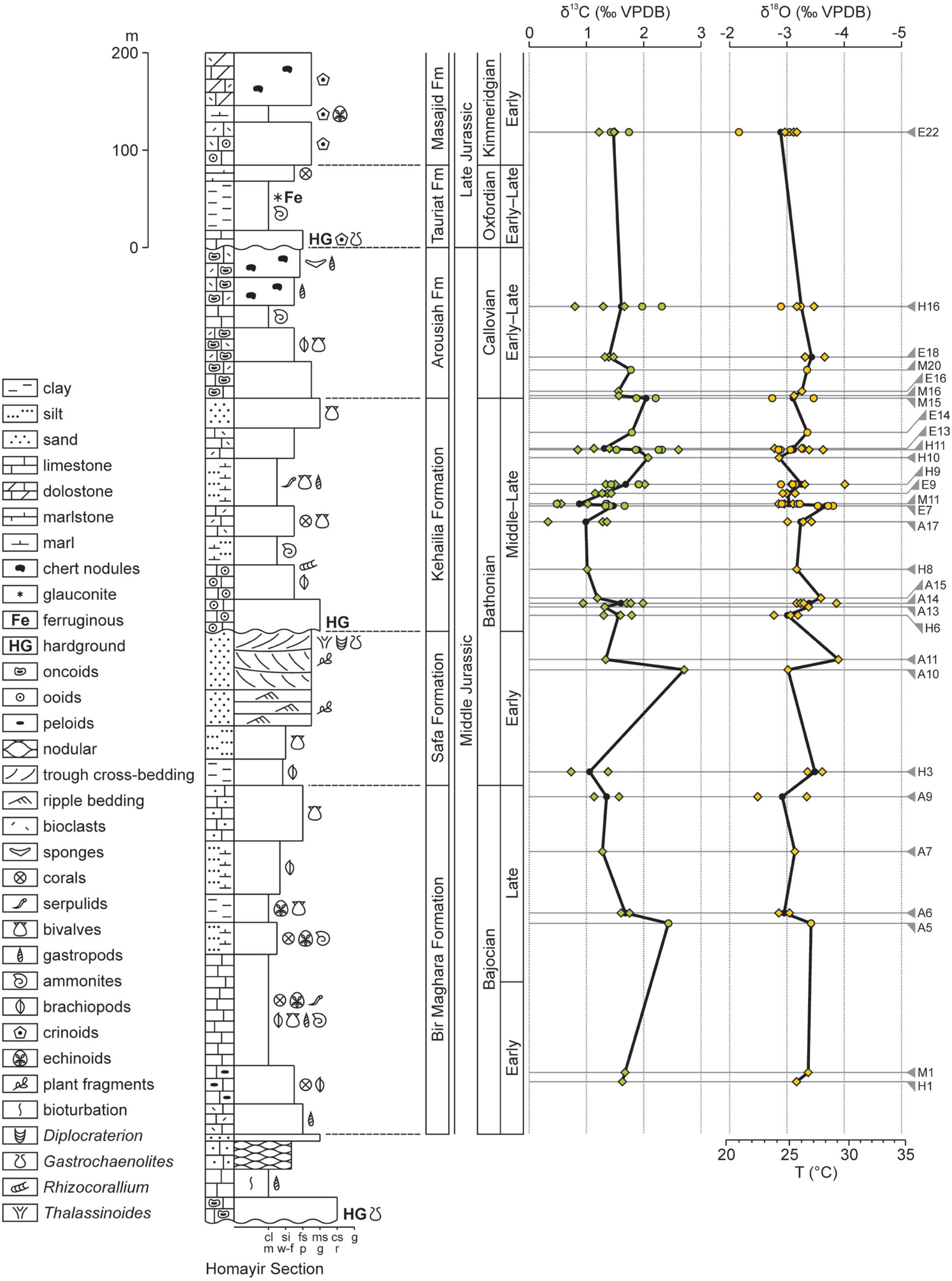

Fig. S4 Results of stable isotope ($\delta^{18}O$, $\delta^{13}C$) analyses of Bajocian-Kimmeridgian bivalve and brachiopod shells from Egypt (modified after Abdelhady, 2014; Alberti et al., 2017). Scale for water temperatures is based on the equation of Anderson and Arthur (1983) and a $\delta^{18}O_{sea}$ value of -1 ‰.

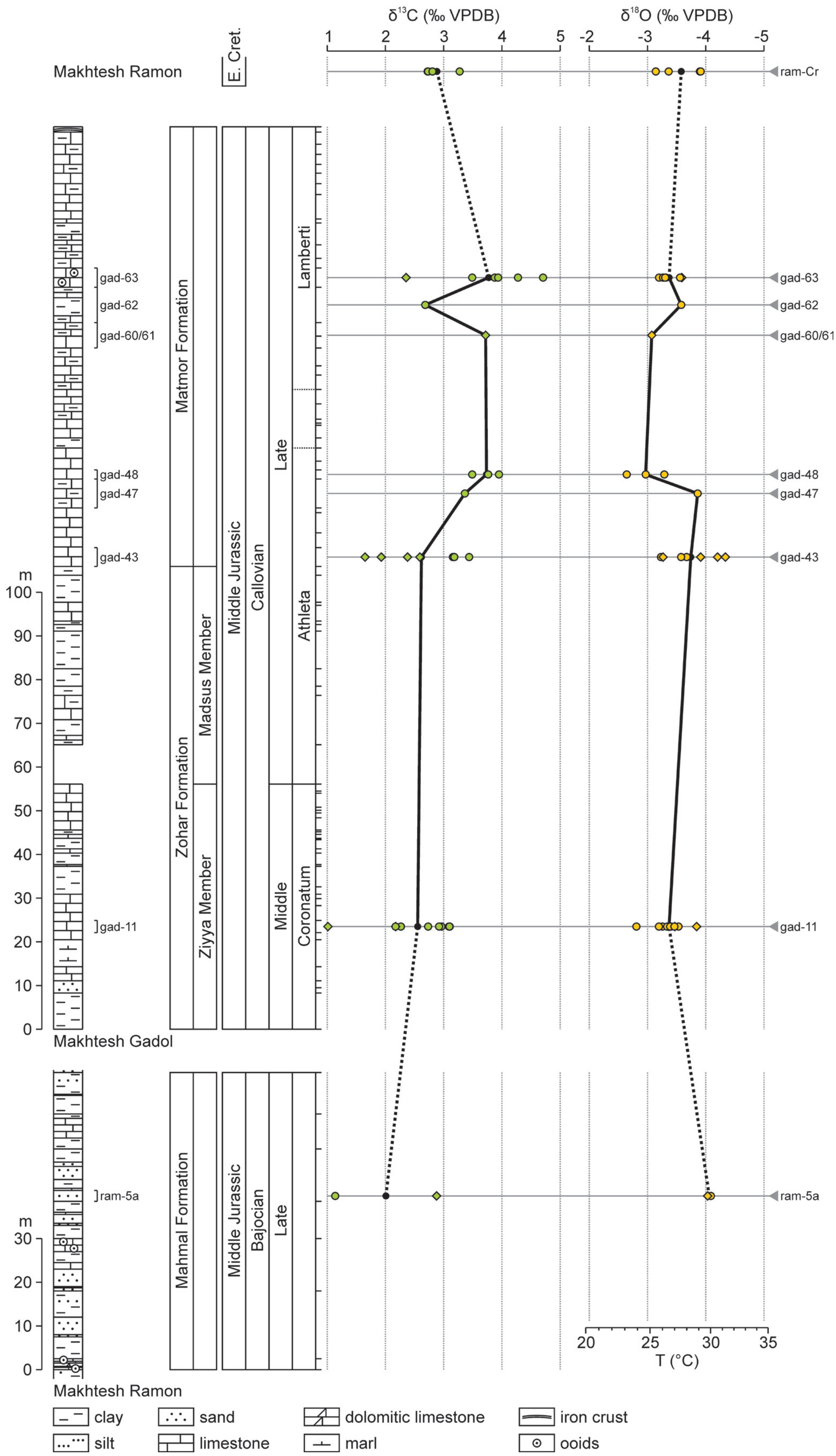

Fig. S5 Results of stable isotope ($\delta^{18}O$, $\delta^{13}C$) analyses of Bajocian-Early Cretaceous bivalve and brachiopod shells from Israel (sections modified after Goldberg, 1963; Parnes, 1981; Hirsch, 2005). Scale for water temperatures is based on the equation of Anderson and Arthur (1983) and a $\delta^{18}O_{sea}$ value of -1 ‰.

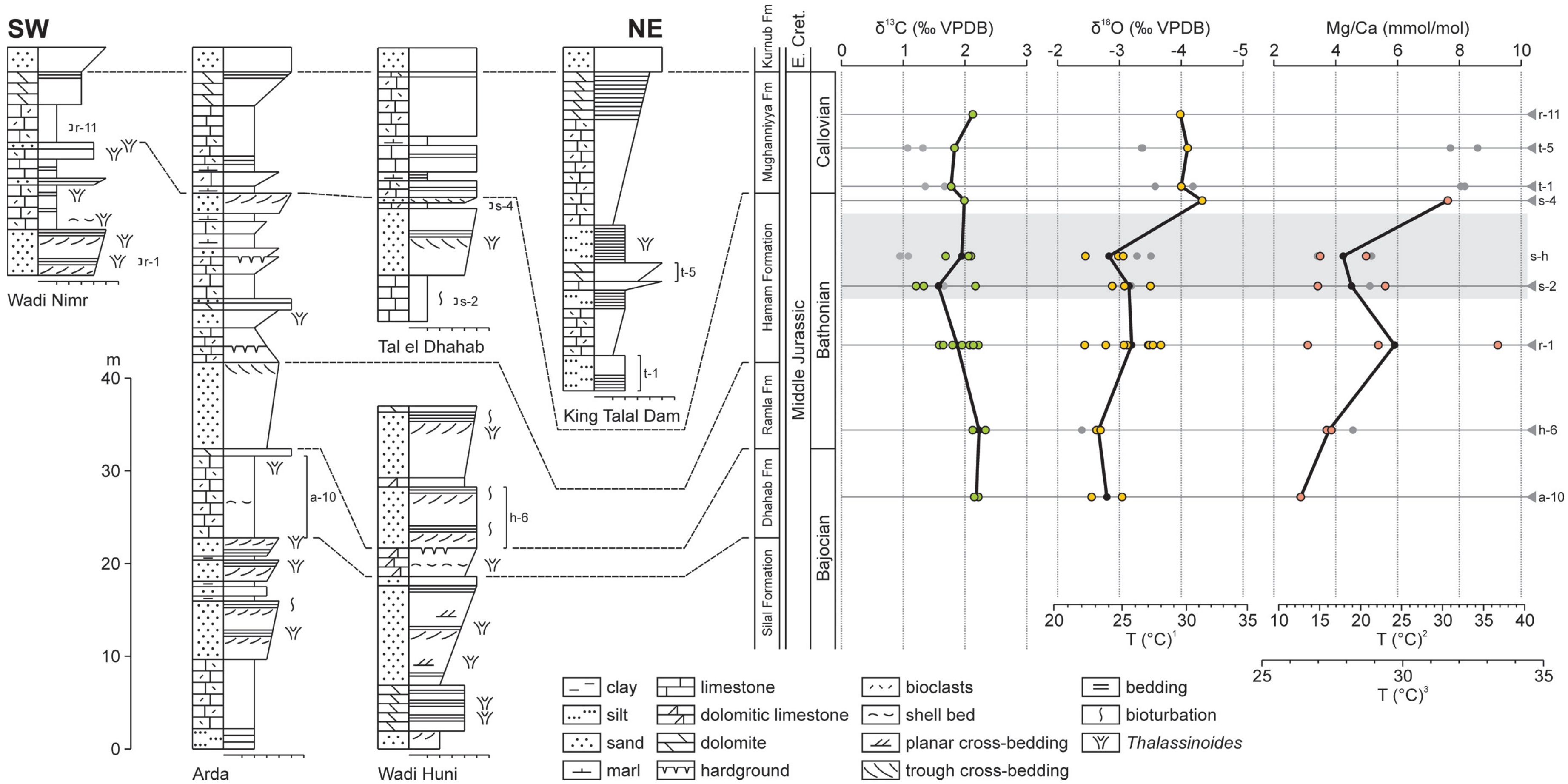

Fig. S6 Results of stable isotope ($\delta^{18}O$, $\delta^{13}C$) and trace element (Mg/Ca) analyses of Bajocian-Callovian bivalve shells from Jordan (sections modified after Ahmad, 1999). Scales for water temperatures are based on (1) the equation of Anderson and Arthur (1983) and a $\delta^{18}O_{sea}$ value of -1 ‰, (2) the equation of Mouchi et al. (2013), or (3) equation (S2) as discussed in the text.

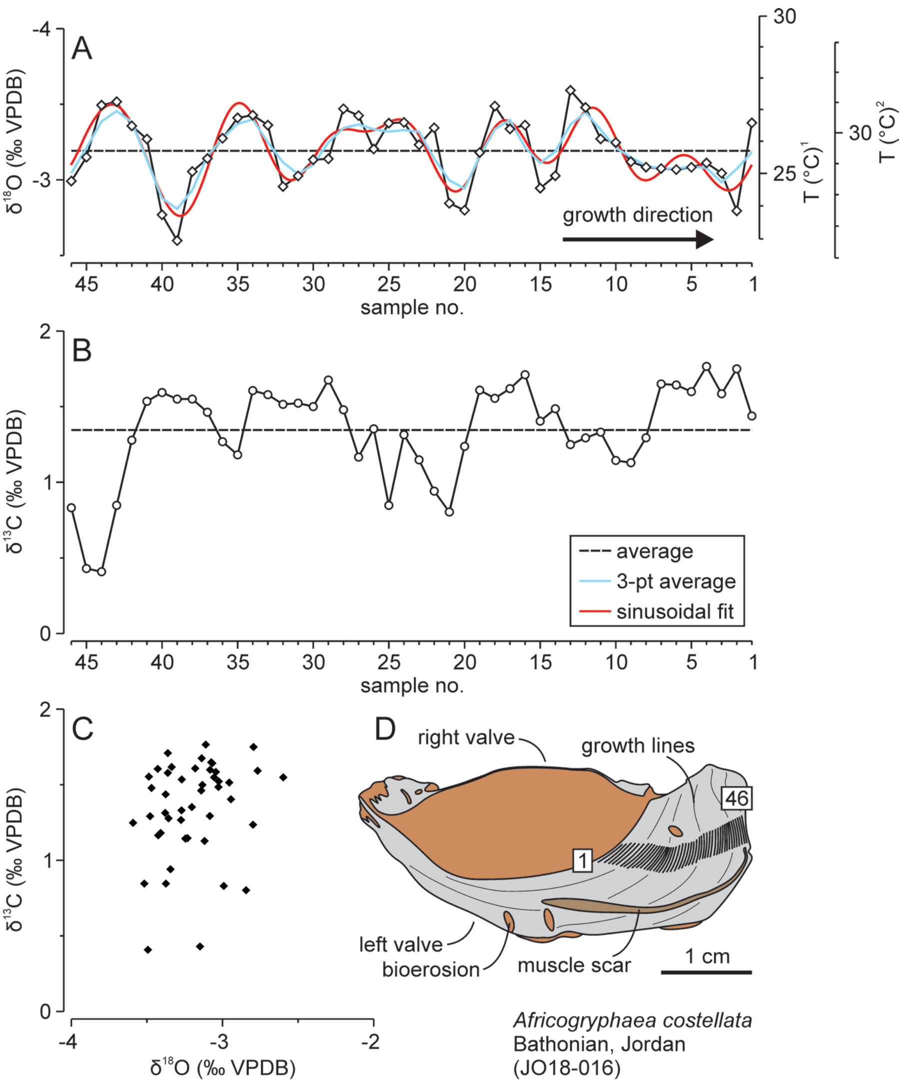

Fig. S7 Results of the high-resolution stable isotope ($\delta^{18}O$, $\delta^{13}C$) analysis of a specimen of *Africogryphaea costellata* from the Bathonian of Jordan. **A.** The measured $\delta^{18}O_{shell}$ values show a cyclic pattern. Scale for water temperatures is based on the equation of Anderson and Arthur (1983) and (1) a $\delta^{18}O_{sea}$ value of -1 ‰ or (2) a $\delta^{18}O_{sea}$ value of -0.23 ‰ corresponding to a palaeolatitude of 1.8 °N. **B.** High-resolution $\delta^{13}C$ data show fluctuating values not corresponding to the cycles in the $\delta^{18}O_{shell}$ values. **C.** Cross-plot of $\delta^{18}O$ versus $\delta^{13}C$ values showing no statistically significant correlation. **D.** Sketch of the used specimen of *Africogryphaea costellata* with the position of the individual samples.

ages (Fig. S6). Their $\delta^{18}O$ values show a more or less steady decrease through time with an average of -2.80 ‰ in the Bajocian and -3.13 ‰ in the Bathonian. Towards the Callovian, $\delta^{18}O$ values decrease again strongly to an average of -4.03 ‰. In contrast, the $\delta^{13}C$ record does not show very strong fluctuations from the Bajocian (average: 2.18 ‰) to the Bathonian (average: 1.88 ‰) and Callovian (average: 1.91 ‰). In addition to stable isotope analyses of individual shells, one oyster shell (*Africogryphaea costellata*; JO18-016) of the Bathonian was used for a high-resolution analysis with 46 samples taken perpendicular to the growth lines (Fig. S7; Table S3). Results from this study show a cyclic pattern in the $\delta^{18}O$ values around an average of -3.19 ‰ (minimum: -3.59 ‰; maximum: -2.60 ‰). A total of five cycles can be identified. The $\delta^{13}C$ values vary around an average of 1.35 ‰ (minimum: 0.41 ‰; maximum: 1.77 ‰), but their fluctuations do not correspond to those in the $\delta^{18}O$ values. In fact, $\delta^{18}O$ and $\delta^{13}C$ values show no correlation (rs = 0.27; p = 0.07).

Table S3 Results of the high-resolution stable isotope ($\delta^{18}O$, $\delta^{13}C$) analysis of a specimen of *Africogryphaea costellata* from the Bathonian of Jordan ([1]Water temperatures based on the equation of Anderson and Arthur (1983) and a $\delta^{18}O_{sea}$ value of -1 ‰, [2]Water temperatures based on the equation of Anderson and Arthur (1983) and a $\delta^{18}O_{sea}$ value of -0.23 ‰ corresponding to a palaeolatitude of 1.8 °N).

sample no.	$\delta^{13}C$	$\delta^{18}O$	T (°C)[1]	T (°C)[2]
JO18-16-1	1.44	-3.38	26.6	30.3
JO18-16-2	1.75	-2.80	23.9	27.5
JO18-16-3	1.59	-3.04	25.0	28.7
JO18-16-4	1.77	-3.11	25.3	29.0
JO18-16-5	1.60	-3.08	25.2	28.9
JO18-16-6	1.64	-3.07	25.1	28.8
JO18-16-7	1.65	-3.08	25.2	28.8
JO18-16-8	1.29	-3.08	25.2	28.9
JO18-16-9	1.13	-3.12	25.4	29.1
JO18-16-10	1.14	-3.25	26.0	29.7
JO18-16-11	1.33	-3.27	26.1	29.8
JO18-16-12	1.29	-3.48	27.1	30.8
JO18-16-13	1.25	-3.59	27.6	31.4
JO18-16-14	1.49	-3.03	24.9	28.6
JO18-16-15	1.40	-2.95	24.5	28.2
JO18-16-16	1.71	-3.36	26.5	30.3
JO18-16-17	1.62	-3.34	26.4	30.1
JO18-16-18	1.56	-3.49	27.1	30.9
JO18-16-19	1.61	-3.18	25.6	29.4
JO18-16-20	1.24	-2.80	23.9	27.5
JO18-16-21	0.80	-2.85	24.1	27.7
JO18-16-22	0.94	-3.34	26.4	30.2
JO18-16-23	1.15	-3.23	25.9	29.6
JO18-16-24	1.31	-3.38	26.6	30.3
JO18-16-25	0.85	-3.38	26.6	30.3
JO18-16-26	1.35	-3.20	25.8	29.5
JO18-16-27	1.17	-3.43	26.8	30.6
JO18-16-28	1.48	-3.47	27.0	30.8
JO18-16-29	1.68	-3.14	25.5	29.2
JO18-16-30	1.50	-3.13	25.4	29.1
JO18-16-31	1.52	-3.03	24.9	28.6
JO18-16-32	1.52	-2.96	24.6	28.3
JO18-16-33	1.58	-3.36	26.5	30.3
JO18-16-34	1.61	-3.43	26.8	30.6
JO18-16-35	1.18	-3.41	26.7	30.5
JO18-16-36	1.27	-3.28	26.1	29.8
JO18-16-37	1.46	-3.14	25.5	29.2
JO18-16-38	1.55	-3.06	25.1	28.7
JO18-16-39	1.55	-2.60	22.9	26.5
JO18-16-40	1.59	-2.77	23.7	27.4
JO18-16-41	1.54	-3.27	26.1	29.8
JO18-16-42	1.28	-3.36	26.5	30.2
JO18-16-43	0.85	-3.52	27.2	31.0
JO18-16-44	0.41	-3.49	27.1	30.9
JO18-16-45	0.43	-3.15	25.5	29.2
JO18-16-46	0.83	-2.99	24.8	28.4

Table S4 Results of trace element (Mg/Ca, Sr/Ca) analyses of well-preserved bivalves from Jordan ([1]Water temperatures based on the equation of Mouchi et al. (2013), [2]Water temperatures based on equation (S2)).

sample no.	taxonomy	Mg/Ca	T (°C)[1]	T (°C)[2]	Sr/Ca
JO18-003	*Gryphaeligmus jabbokensis*	3.42	14.8	27.0	0.73
JO18-004	*Gryphaeligmus jabbokensis*	5.60	23.0	29.4	0.74
JO18-018	*Africogryphaea costellata*	3.49	15.1	27.1	0.72
JO18-019	*Gryphaeligmus jabbokensis*	7.63	30.6	31.6	0.85
JO18-023	*Africogryphaea costellata*	4.98	20.7	28.7	0.58
JO18-024	*Africogryphaea costellata*	3.09	13.5	26.6	0.70
JO18-027	*Africogryphaea costellata*	9.25	36.7	33.4	2.67
JO18-028	*Africogryphaea costellata*	2.87	12.7	26.4	0.82
JO18-033	*Africogryphaea costellata*	3.86	16.4	27.5	0.71
JO18-034	*Africogryphaea costellata*	3.71	15.9	27.3	0.75
JO18-032	*Gryphaeligmus jabbokensis*	5.38	22.2	29.1	0.80

Trace element analyses

Eleven seemingly well-preserved shells of the bivalves *Africogryphaea costellata* and *Gryphaeligmus jabbokensis* from Jordan were analysed for their Mg/Ca- and Sr/Ca-ratios (Table S4). Measured Mg/Ca-ratios are between 2.87 and 9.25 mmol/mol and Sr/Ca-ratios vary between 0.58 and 0.85 mmol/mol with one outlier at 2.67 mmol/mol. Mg/Ca-ratios show a statistically significant negative correlation with $\delta^{18}O$ values (rs = -0.75; p = 0.007), whether considered individually for each species or together (Fig. S2B). It should be noted, however, that in the case of *Africogryphaea costellata*, this correlation strongly depends on one sample with (suspiciously?) high Sr/Ca- and Mg/Ca-ratios. Similar to the $\delta^{18}O$ values, Mg/Ca-ratios exhibit a prominent trend through time. Their record starts with a minimum of 2.87 mmol/mol in the Bajocian, increasing to higher values over most of the Bathonian (average: 5.04 mmol/mol), before reaching a Mg/Ca-ratio of 7.63 mmol/mol just before the Bathonian-Callovian boundary (Fig. S6).

Water temperatures of the individual study areas

The reconstruction of absolute water temperatures based on $\delta^{18}O_{shell}$ values depends on a number of variables. Diagenetic alteration leading to a change in the stable isotope composition, vital effects of the used fossil taxa, and environmental factors are the most prominent. As explained above, steps have been taken to identify poorly preserved fossils in the collections. Furthermore, sedimentology and palaeoecology show that the study sites represent fully-marine settings above the thermocline, limiting the potential influence of salinity changes (e.g., via river discharge). Some climate models reconstructed seasonal rainfall patterns (and possibly upwelling) along the northern coast of Gondwana during the Jurassic which could influence local $\delta^{18}O_{sea}$ values (e.g., Price et al., 1995; Sellwood and Valdes, 2006). In contrast, high-resolution stable isotope analyses conducted on bivalve shells from Jordan and Egypt (compare Fig. S7 and Alberti et al., 2017) show very weak seasonal changes in stable isotope values ($\delta^{18}O$ and $\delta^{13}C$). These results disagree with the presence of strong seasonal rainfall or upwelling patterns which would be expected to result in much stronger fluctuations (compare Sadatzki et al., 2019). The location of the study sites in direct contact with the Tethys Ocean also suggest that conditions corresponded to an open-ocean setting. Finally, previous studies showed very similar stable isotope values for bivalves and rhynchonellid brachiopods sampled from the same horizons supporting the validity of combining data of both taxonomic groups (e.g., Alberti et al., 2012a).

The following water temperatures were reconstructed with the equation of Anderson and Arthur (1983) and a $\delta^{18}O_{sea}$ value determined with equation (4) for the individual palaeolatitudes (Table S2). There is a series of other equations available in literature (e.g., Epstein et al., 1953; Craig, 1965; Leng and Marshall, 2004; Takayanagi et al., 2013; Brand et al., 2013), but for the relatively low $\delta^{18}O_{shell}$ values recorded from the equatorial regions in this study, results are quite comparable (compare Fig. S8). Therefore, we decided to apply the equation of Anderson and Arthur (1983), which is very widely used in literature and thereby facilitates comparisons between articles.

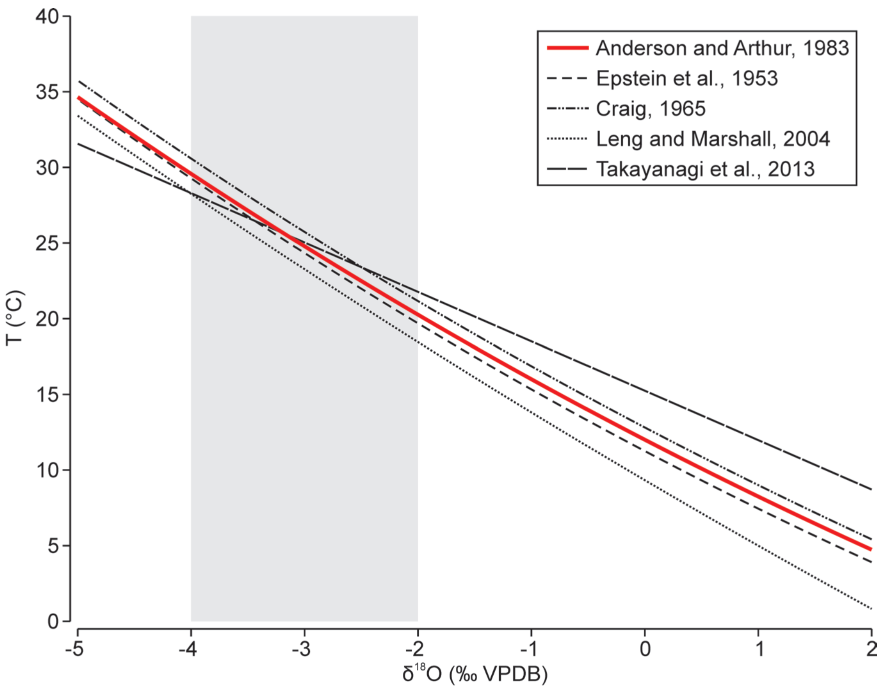

Fig. S8 A comparison of different equations used for temperature reconstructions based on stable oxygen isotope values shows that results are comparatively similar for lower $\delta^{18}O_{shell}$ values (=higher water temperatures), but differ more strongly at higher $\delta^{18}O_{shell}$ values (=lower water temperatures). Most samples from the equatorial study sites show $\delta^{18}O_{shell}$ values between -2 and -4 ‰. In this range, the widely used equation of Anderson and Arthur (1983) seems to be a reasonable fit. Temperatures in the graph were calculated for a $\delta^{18}O_{sea}$ value of -1 ‰.

Furthermore, temperatures reconstructed based on Anderson and Arthur (1983) fall well within the center compared to the other equations. Using a different equation would not change the conclusions of the study markedly.

Only four well-preserved shells were available from Morocco (palaeolatitude 26-28 °N) which point to water temperatures around 28.0 °C in the ?Toarcian-Aalenian, 23.9 °C in the Bajocian, 22.7 °C in the Callovian, and 22.7 °C in the Oxfordian. This seems to agree with reconstructions by Martin-Garin et al. (2010) for the Kimmeridgian of Morocco, who proposed water temperatures of around 24.6 °C based on stable oxygen isotope analyses of three brachiopods. However, Martin-Garin et al. (2010) used a $\delta^{18}O_{sea}$ value of -1.2 ‰ for their temperature calculations, which seems to be too low for a palaeolatitude of around 26 °N. If their original data is used with the method suggested within the present study, the Kimmeridgian water temperatures were much warmer (around an average of 30.6 °C).

Stable isotope analyses of 41 Callovian brachiopod shells of Tunisia (palaeolatitude 13-14 °N) point to water temperatures around an average of 28.3 °C (range: 24.0 to 33.6 °C). Water temperatures fluctuate considerably throughout the Callovian, but do not show a prominent long-term trend (Fig. 3A).

Results based on 73 well-preserved brachiopod and bivalve shells of Egypt (palaeolatitude 2-4 °N) indicate water temperatures around 29.3 °C in the Bajocian (range: 26.4 to 30.9 °C), 29.9 °C in the Bathonian (range: 27.7 to 33.9 °C), 30.2 °C in the Callovian (range: 27.6 to 32.1 °C), and 28.2 °C in the Kimmeridgian (range: 24.7 to 29.6 °C). Temperatures fluctuate slighty through time, but do not show prominent long-term trends (Fig. 3B; Alberti et al., 2017).

Thirty-five brachiopod and bivalve shells from Israel (palaeolatitude 2-3 °N) were analysed with their $\delta^{18}O_{shell}$ values translating into water temperatures around 34.0 °C in the Bajocian (range: 33.9 to 34.1 °C), 30.9 °C in the Callovian (range: 27.0 to 35.5 °C), and 31.4 °C in the Early Cretaceous (range: 29.2 to 33.1 °C). While the average temperatures seem to show a cooling from the Bajocian towards the Callovian (Fig. 3C), it should be noted that the Bajocian is represented only by two shells, which hinders the reliable recognition of long-term trends.

Stable isotope analyses of 22 bivalve shells from Jordan (palaeolatitude 1-2 °N) point to water temperatures around 27.5 °C in the Bajocian (range: 26.3 to 28.7 °C), 29.1 °C in the Bathonian (range: 25.8 to 35.2 °C), and 33.6 °C in the Callovian (range: 33.4 to 34.0 °C). Despite the limited number of samples, the results seem to indicate a warming in the study area starting in the latest Bathonian (Fig. 3D). This is supported by the measured Mg/Ca-ratios, which show a statistically significant, negative correlation to the $\delta^{18}O_{shell}$ values (Fig. S2B; Table S4). Mg/Ca-ratios of bivalve shells have been studied for their potential as temperature proxies, but their relationship to water temperatures seem to vary strongly between different species (e.g., Surge and Lohmann, 2008; Mouchi et al., 2013; Bougeois et al., 2016; Tynan et al., 2017). Mouchi et al. (2013) developed the following equation for the oyster *Crassostrea gigas* to calculate water temperatures based on Mg/Ca-ratios:

(S1) $T\ (°C) = 3.77 * Mg/Ca + 1.88$

However, if this equation is used on the present dataset of *Africogryphaea costellata* and *Gryphaeligmus jabbokensis*, the reconstructed water temperatures are mostly too low (range: 12.7 to 30.6 °C; Fig. S6). The correlation between Mg/Ca-ratios and $\delta^{18}O_{shell}$ values in the current dataset can also be used to establish a relationship with water temperatures reconstructed from the oxygen isotopes (Fig. S6):

(S2) $T\ (°C) = 1.0973 * Mg/Ca + 23.232$

This relationship differs slightly, if equations are formed separately for both species, but the sample number is too low to come to a definite conclusion. Nevertheless, since both species are common in the Jurassic strata of northern Africa and western Asia, it might be useful to study the relationship between their Mg/Ca-ratios and $\delta^{18}O_{shell}$ values further in the future.

One specimen of *Africogryphaea costellata* from the Bathonian of Jordan was sampled at high resolution. Its shell recorded cyclic fluctuations around an average of 29.4 °C believed to be caused by seasonal weather changes (Fig. S7A). If explained only by water temperatures, the $\delta^{18}O_{shell}$ values translate into temperature between 26.5 and 31.4 °C. A seasonality of around 5 °C is slightly higher than that reconstructed for the Bathonian of Egypt by Alberti et al. (2017). Strong seasonal rainfall or upwelling patterns would have led to stronger changes in the $\delta^{18}O_{shell}$ values, but it cannot be excluded that minor seasonal changes in local $\delta^{18}O_{sea}$ values might have contributed to the signal (compare Moore et al., 1992).

Additional literature

Length-restrictions do not allow the citation of all studies connected with the conducted research within the article itself, therefore some additional literature will be mentioned in the following:

- Studies mentioning the Jurassic world being warmer than today with weak latitudinal temperature gradients, no polar glaciations, and/or a lack of major perturbations include Moore et al. (1992), Valdes and Sellwood (1992), Hallam (2001), and Sellwood and Valdes (2006). In contrast, some articles mentioning phases of polar glaciations in the Jurassic include Price (1999) and Dromart et al. (2003). In particular, the glaciation at the Callovian-Oxfordian boundary proposed by Dromart et al. (2003) has been debated in literature (e.g., Wierzbowski et al., 2009).
- There is a substantial amount of literature on stable isotope research connected to temperature reconstructions including for the Jurassic world. These studies concentrate on methodology, regional temperature developments, and/or global temperature changes. Some of these, which were considered, but ultimately not included in the discussion are Urey et al. (1951), Epstein et al. (1951), Podlaha et al. (1998), Wierzbowski (2002, 2004), Gröcke et al. (2003), Fürsich et al. (2005), Brigaud et al. (2008), Wierzbowski et al. (2009), Mutterlose et al. (2010), Alberti et al. (2012b, 2013, 2019), Martinez and Dera (2015), Ullmann et al. (2016), and Danise et al. (2020).
- Other methods applied for temperature reconstructions in the Jurassic include clumped isotope

analyses and the TEX_{86} palaeothermometer. Commonly, TEX_{86}-data result in temperatures warmer than those from the „classic" stable oxygen isotopes. This has been interpreted in different ways, either supporting or discounting the applicability of the TEX_{86} proxy. In general, TEX_{86}-data might indicate warmer surface water temperatures compared to stable oxygen isotopes of bottom-dwelling or deep-swimming organisms, but the exact calibration method for TEX_{86} is also debated and might influence absolute temperature reconstructions (compare Jenkyns et al., 2012; Vickers et al., 2019; Price et al., 2020). Clumped isotope analyses are still very few for the Jurassic world and connected with a number of uncertainties. Results of Wierzbowski et al. (2018) for western Russia and Vickers et al. (2020) for Scotland point to fluctuating $\delta^{18}O_{sea}$ values due to the complex European palaeogeography (including changes in ocean currents and salinity fluctuations). Their reconstructed $\delta^{18}O_{sea}$ values span a wide spectrum, but do not necessarily correspond to open-ocean settings. Similarly, Vickers et al. (2019) used clumped isotope analyses on samples from the Falkland Plateau, but resulting $\delta^{18}O_{sea}$ values point to a restricted situation for their study area. Finally, Price et al. (2020) used clumped isotope analyses to reconstruct latitudinal gradients in the Early Cretaceous. While they reconstructed a latitudinal $\delta^{18}O_{sea}$ gradient almost parallel to the modern-day one, absolute $\delta^{18}O_{sea}$ values are much higher and therefore almost unrealistic as they would require enormous polar ice shields. The reasons for these high $\delta^{18}O_{sea}$ values reconstructed via clumped isotope analyses are still debated, but might be caused by the used calibration method and require additional research.

- The discussion on the ecological impact of the proposed elevated water temperatures along the equator during the Jurassic had to be kept very short, but literature focusing on this aspect is also relatively sparse yet. Some studies showing the importance of water temperatures on marine diversities include Roy et al. (1998), Figueira and Booth (2010), and Yamano et al. (2011). Additional articles including data on Jurassic faunas potentially pointing to generally elevated temperatures during the Jurassic or comparatively low diversities at low latitudes include Tintant (1987), Legarreta (1991), Fischer et al. (2001), and Leinfelder et al. (2005).

References

Abdelhady, A.A. 2014. Palaeoenvironments and palaeoecology of the Middle and Upper Jurassic succession of Gebel Maghara (Sinai). Universität Erlangen-Nürnberg, Germany, 182 p. (Unpublished PhD thesis).

Abdelhady, A.A., Fürsich, F.T. 2014. Macroinvertebrate palaeo-communities from the Jurassic succession of Gebel Maghara (Sinai, Egypt). – Journal of African Earth Sciences 97: 173-193.

Abdelhady, A.A., Fürsich, F.T. 2015a. Quantitative biostratigraphy of the Middle to Upper Jurassic strata of Gebel Maghara (Sinai, Egypt). – Newsletters on Stratigraphy 48: 23-46.

Abdelhady, A.A., Fürsich, F.T. 2015b. Sequence architecture of a Jurassic ramp succession from Gebel Maghara (North Sinai, Egypt): implications for eustasy. – Journal of Palaeogeography 4: 305-330.

Abdelhady, A.A., Fürsich, F.T. 2015c. Palaeobiogeography of the Bajocian-Oxfordian macrofauna of Gebel Maghara (North Sinai, Egypt): implications for eustasy and basin topography. – Palaeogeography, Palaeoclimatology, Palaeoecology 417: 261-273.

Ahmad, F. 1999. Middle Jurassic macroinvertebrates from northwestern Jordan. – Beringeria 23: 3-46.

Alberti, M., Fürsich, F.T., Pandey, D.K. 2012a. The Oxfordian stable isotope record ($\delta^{18}O$, $\delta^{13}C$) of belemnites, brachiopods, and oysters from the Kachchh Basin (western India) and its potential for palaeoecologic, palaeoclimatic, and palaeogeographic reconstructions. – Palaeogeography, Palaeoclimatology, Palaeoecology 344-345: 49-68.

Alberti, M., Fürsich, F.T., Pandey, D.K., Ramkumar, M. 2012b. Stable isotope analyses of belemnites from the Kachchh Basin, western India: paleoclimatic implications for the Middle to Late Jurassic transition. – Facies 58: 261-278.

Alberti, M., Fürsich, F.T., Pandey, D.K. 2013. Seasonality in low latitudes during the Oxfordian (Late Jurassic) reconstructed via high-resolution stable isotope analysis of the oyster *Actinostreon marshi* (J. Sowerby, 1814) from the Kachchh Basin, western India. – International Journal of Earth Sciences 102: 1321-1336.

Alberti, M., Fürsich, F.T., Abdelhady, A.A., Andersen, N. 2017. Middle to Late Jurassic equatorial seawater temperatures and latitudinal temperature gradients based on stable isotopes of brachiopods and oysters from Gebel Maghara, Egypt. – Palaeogeography, Palaeoclimatology, Palaeoecology 468: 301-313.

Alberti, M., Fürsich, F.T., Andersen, N. 2019. First steps in reconstructing Early Jurassic sea water temperatures in the Andean Basin of northern Chile based on stable isotope analyses of oyster and brachiopod shells. – Journal of Palaeogeography 8: 33.

Anderson, T.F., Arthur, M.A. 1983. Stable isotopes of oxygen and carbon and their application to sedimentological and paleoenvironmental problems. – In: Arthur, M.A., Anderson, T.F., Kaplan, I.R., Veizer, J., Land, L. (Eds.), Stable isotopes in sedimentary geology. SEPM Short Course, 1-151.

Arabas, A. 2016. Middle-Upper Jurassic stable isotope records and seawater temperature variations: New palaeoclimate data from marine carbonate and belemnite rostra (Pieniny Klippen Belt, Carpathians). – Palaeogeography, Palaeoclimatology, Palaeoecology 446: 284-294.

Bougeois, L., de Rafélis, M., Reichart, G.-J., de Nooijer, L.J., Dupont-Nivet, G. 2016. Mg/Ca in fossil oyster shells as palaeotemperature proxy, an example from the Palaeogene of Central Asia. – Palaeogeography, Palaeoclimatology, Palaeoecology 441: 611-626.

Brand, U., Azmy, K., Bitner, M.A., Logan, A., Zuschin, M., Came, R., Ruggiero, E. 2013. Oxygen isotopes and $MgCO_3$ in brachiopod calcite and a new paleotemperature equation. – Chemical Geology 359: 23-31.

Brigaud, B., Pucéat, E., Pellenard, P., Vincent, B., Joachimski, M.M. 2008. Climatic fluctuations and seasonality during the Late Jurassic (Oxfordian-Early Kimmeridgian) inferred from $\delta^{18}O$ of Paris Basin oyster shells. – Earth and Planetary Science Letters 273: 58-67.

Craig, H. 1965. The measurement of oxygen isotope paleotemperatures. – In: Tongiorgi, E. (Ed.), Stable isotopes in oceanographic studies and paleotemperatures. Consiglio Nazionale delle Ricerche Laboratorio di Geologia Nucleare, Pisa, 161-182.

Danise, S., Price, G.D., Alberti, M., Holland, S.M. 2020. Isotopic evidence for partial geochemical decoupling between a Jurassic epicontinental sea and the open ocean. – Gondwana Research 82: 97-107.

Dera, G., Brigaud, B., Monna, F., Laffont, R., Pucéat, E., Deconinck, J.-F., Pellenard, P., Joachimski, M.M., Durlet, C. 2011. Climatic ups and downs in a disturbed Jurassic world. – Geology 39: 215-218.

de Villiers, S., Greaves, M., Elderfield, H. 2002. An intensity ratio calibration method for the accurate determination of Mg/Ca and Sr/Ca of marine carbonates by ICP-AES. – Geochemistry Geophysics Geosystems 3 (1).

Dromart, G., Garcia, J.-P., Picard, S., Atrops, F., Lécuyer, C., Sheppard, S.M.F. 2003. Ice age at the Middle-Late Jurassic transition? – Earth and Planetary Science Letters 213: 205-220.

Dubar, G. 1967. Brachiopodes jurassiques du Sahara Tunisien. – Annales de Paléontologie (Invertébrés) 53: 31-71.

Epstein, S., Buchsbaum, R., Lowenstam, H.A., Urey, H.C. 1951. Carbonate-water isotopic temperature scale. – Geological Society of America Bulletin 62: 417-426.

Epstein, S., Buchsbaum, R., Lowenstam, H.A. 1953. Revised carbonate-water isotopic temperature scale. – Geological Society of America Bulletin 64: 1315-1325.

Feldman, H.R., Owen, E.F., Hirsch, F. 2001. Brachiopods from the Jurassic (Callovian) of Hamakhtesh Hagadol (Kurnub Anticline), southern Israel. – Palaeontology 44: 637-658.

Feldman, H.R., Schemm-Gregory, M., Ahmad, F., Wilson, M.A. 2012. Jurassic rhynchonellide brachiopods from the Jordan Valley. – Acta Palaeontologica Polonica 57: 191-204.

Feldman, H.R., Schemm-Gregory, M., Ahmad, F., Wilson, M.A. 2014. A Jurassic (Bathonian-Callovian) Daghanirhynchia brachiopod fauna from Jordan. – Geologica Acta 12: 1-18.

Figueira, W.F., Booth, D.J. 2010. Increasing ocean temperatures allow tropical fishes to survive overwinter in temperate waters. – Global Change Biology 16: 506-516.

Fischer, J.-C., Le Nindre, Y.-M., Manivit, J., Vaslet, D. 2001. Jurassic gastropod faunas of central Saudi Arabia. – GeoArabia 6: 63-100

Fürsich, F.T., Singh, I.B., Joachimski, M., Krumm, S., Schlirf, M., Schlirf, S. 2005. Palaeoclimatic reconstructions of the Middle Jurassic of Kachchh (western India): an integrated approach based on palaeoecological, oxygen isotopic, and clay mineralogical data. – Palaeogeography, Palaeoclimatology, Palaeoecology 217: 289-309.

Goldberg, M. 1963. Reference section of Jurassic sequence exposed in Hamakhtesh Hagadol (Kurnub anticline). Unpublished Internal Report Oil Division, Geological Survey of Israel, Jerusalem, 50 p.

Greaves, M., Caillon, N., Rebaubier, H., Bartoli, G., Bohaty, S., Cacho, I., Clarke, L., Cooper, M., Daunt, C., Delaney, M., deMenocal, P., Dutton, A., Eggins, S., Elderfield, H., Garbe-Schoenberg, D., Goddard, E., Green, D., Groeneveld, J., Hastings, D., Hathorne, E., Kimoto, K., Klinkhammer, G., L. Labeyrie, L., Lea, D.W., Marchitto, T., Martínez-Botí, M.A., Mortyn, P.G., Ni, Y., Nuernberg, D., Paradis, G., Pena, L., Quinn, T., Rosenthal, Y., Russell, A., Sagawa, T., Sosdian, S., Stott, L., Tachikawa, K., Tappa, E., Thunell, R., Wilson, P.A. 2008. Interlaboratory comparison study of calibration standards for foraminiferal Mg/Ca thermometry. – Geochemistry Geophysics Geosystems 9 (8).

Gröcke, D.R., Price, G.D., Ruffell, A.H., Mutterlose, J., Baraboshkin, E. 2003. Isotopic evidence for Late Jurassic-Early Cretaceous climate change. – Palaeogeography, Palaeoclimatology, Palaeoecology 202: 97-118.

Hallam, A. 2001. A review of the broad pattern of Jurassic sea-level changes and their possible causes in the light of current knowledge. – Palaeogeography, Palaeoclimatology, Palaeoecology 167: 23-37.

Hathorne, E.C., Gagnon, A., Felis, T., Adkins, J., Asami, R., Boer, W., Caillon, N., Case, D., Cobb, K.M., Douville, E., deMenocal, P., Eisenhauer, A., Garbe-Schönberg, D., Geibert, W., Goldstein, S., Hughen, K., Inoue, M., Kawahata, H., Kölling, M., Cornec, F.L., Linsley, B.K., McGregor, H.V., Montagna, P., Nurhati, I.S., Quinn, T.M., Raddatz, J., Rebaubier, H., Robinson, L., Sadekov, A., Sherrell, R., Sinclair, D., Tudhope, A.W., Wei, G., Wong, H., Wu, H.C., You, C.-F. 2013. Interlaboratory study for coral Sr/Ca and other element/Ca ratio measurements. – Geochemistry Geophysics Geosystems 14 (9): 3730-3750.

Hirsch, F. 2005. Chapter 18A. Introduction to the stratigraphy of Israel. – In: Hall, J.K., Krasheninnikov, V.A., Hirsch, F., Benjamini, C., Flexer, A. (Eds.), Geological framework of the Levant, Volume II: The Levantine Basin and Israel. Historical Productions-Hall, 269-282.

Hodgson, W.A. 1966. Carbon and oxygen isotope ratios in diagenetic carbonates from marine sediments. – Geochimica et Cosmochimica Acta 30: 1223-1233.

Hoffmann, R., Stevens, K. 2019. The palaeobiology of belemnites – foundation for the interpretation of rostrum geochemistry. – Biological Reviews.

Holzapfel, S. 1998. Palökologie benthischer Faunengemeinschaften und Taxonomie der Bivalven im Jura von Südtunesien. – Beringeria 22: 3-199.

Hudson, J.D. 1977. Stable isotopes and limestone lithification. – Journal of the Geological Society London 133: 637-660.

Huyghe, D., Emmanuel, L., de Rafelis, M., Renard, M., Ropert, M., Labourdette, N., Lartaud, F. 2020. Oxygen isotope disequilibrium in the juvenile portion of oyster shells biases seawater temperature reconstructions. – Estuarine, Coastal and Shelf Science 240: 106777.

Jenkyns, H.C., Schouten-Huibers, L., Schouten, S., Sinninghe-Damsté, J.S. 2012. Warm Middle Jurassic-Early Cretaceous high-latitude sea-surface temperatures from the Southern Ocean. – Climate of the Past 8: 215-226.

Kent, D.V., Irving, E. 2010. Influence of inclination error in sedimentary rocks on the Triassic and Jurassic apparent pole wander path for North America and implications for Cordilleran tectonics. – Journal of Geophysical Research 115: B10103.

Korte, C., Hesselbo, S.P., Ullmann, C.V., Dietl, G., Ruhl, M., Schweigert, G., Thibault, N. 2015. Jurassic climate mode governed by ocean gateway. – Nature Communications 6: 10015.

Legarreta, L. 1991. Evolution of a Callovian-Oxfordian carbonate margin in the Neuquén Basin of west-central Argentina: facies, architecture, depositional sequences and global sea-level changes. – Sedimentary Geology 70: 209-240.

Leinfelder, R.R., Schlagintweit, F., Werner, W., Ebli, O., Nose, M., Schmid, D.U., Hughes, G.W. 2005. Significance of stromatoporoids in Jurassic reefs and carbonate platforms – concepts and implications. – Facies 51: 287-325.

Leng, M.J., Marshall, J.D. 2004. Palaeoclimate interpretation of stable isotope data from lake sediment archives. – Quaternary Science Reviews 23: 811-831.

Martinez, M., Dera, G. 2015. Orbital pacing of carbon fluxes by a ~9-My eccentricity cycle during the Mesozoic. – Proceedings of the National Academy of Sciences 112: 12604-12609.

Martin-Garin, B., Lathuilière, B., Geister, J., Ramseyer, K. 2010. Oxygen isotopes and climatic control of Oxfordian coral reefs (Jurassic, Tethys). – Palaios 25: 721-729.

Martin-Garin, B., Lathuilière, B., Geister, J. 2012. The shifting biogeography of reef corals during the Oxfordian (Late Jurassic). A climatic control? – Palaeogeography, Palaeoclimatology, Palaeoecology 365-366: 136-153.

Moore, G.T., Hayashida, D.N., Ross, C.A., Jacobson, S.R. 1992. Paleoclimate of the Kimmeridgian/Tithonian (Late Jurassic) world: I. Results using a general circulation model. – Palaeogeography, Palaeoclimatology, Palaeoecology 93: 113-150.

Mouchi, V., de Rafélis, M., Lartaud, F., Fialin, M., Verrecchia, E. 2013. Chemical labelling of oyster shells used for time-calibrated high-resolution Mg/Ca ratios: A tool for estimation of past seasonal temperature variations. – Palaeogeography, Palaeoclimatology, Palaeoecology 373: 66-74.

Mutterlose, J., Malkoc, M., Schouten, S., Sinninghe Damsté, J.S., Forster, A. 2010. TEX_{86} and stable $\delta^{18}O$ paleothermometry of Early Cretaceous sediments: implications for belemnite ecology and paleotemperature proxy application. – Earth and Planetary Science Letters 298: 286-298.

Nelson, C.S., Smith, A.M. 1996. Stable oxygen and carbon isotope compositional fields for skeletal and diagenetic components in New Zealand Cenozoic nontropical carbonate sediments and limestones: a synthesis and review. – New Zealand Journal of Geology and Geophysics 39: 93-107.

Parnes, A. 1981. Biostratigraphy of the Mahmal Formation (Middle and Upper Bajocian) in Makhtesh Ramon (Negev, southern Israel). – Israel Geological Survey, Bulletin 74: 1-55.

Podlaha, O.G., Mutterlose, J., Veizer, J. 1998. Preservation of $\delta^{18}O$ and $\delta^{13}C$ in belemnite rostra from the Jurassic/Early Cretaceous successions. – American Journal of Science 298: 324-347.

Price, G.D. 1999. The evidence and implications of polar ice during the Mesozoic. – Earth-Science Reviews 48: 183-210.

Price, G.D., Sellwood, B.W. 1997. "Warm" palaeotemperatures from high Late Jurassic palaeolatitudes (Falkland Plateau): Ecological, environmental or diagentic controls? – Palaeogeography, Palaeoclimatology, Palaeoecology 129: 315-327.

Price, G.D., Sellwood, B.W., Valdes, P.J. 1995. Sedimentological evaluation of general circulation model simulations for the „greenhouse" Earth: Cretaceous and Jurassic case studies. – Sedimentary Geology 100: 159-180.

Price, G.D., Hart, M.B., Wilby, P.R., Page, K.N. 2015. Isotopic analysis of Jurassic (Callovian) mollusks from the Christian Malford Lagerstätte (UK): Implications for ocean water temperature estimates based on belemnoids. – Palaios 30: 645-654.

Price, G.D., Bajnai, D., Fiebig, J. 2020. Carbonate clumped isotope evidence for latitudinal seawater temperature gradients and the oxygen isotope composition of Early Cretaceous seas. – Palaeogeography, Palaeoclimatology, Palaeoecology 552: 109777.

Roy, K., Jablonski, D., Valentine, J.W., Rosenberg, G. 1998. Marine latitudinal diversity gradients: tests of causal hypotheses. – Proceedings of the National Academy of Sciences 95: 3699-3702.

Sadatzki, H., Alberti, M., Garbe-Schönberg, D., Andersen, N., Strey, P., Fortunato, H., Andersson, C., Schäfer, P. 2019. Paired Li/Ca and $\delta^{18}O$ peaks in bivalve shells from the Gulf of Panama mark seasonal coastal upwelling. – Chemical Geology 529: 119295.

Schrag, D.P. 1999. Rapid analysis of high-precision Sr/Ca ratios in corals and other marine carbonates. – Paleoceanography 14: 97-102.

Sellwood, B.W., Valdes, P.J. 2006. Mesozoic climates: general circulation models and the rock record. – Sedimentary Geology 190: 269-287.

Surge, D., Lohmann, K.C. 2008. Evaluating Mg/Ca ratios as a temperature proxy in the estuarine oyster, *Crassostrea virginica*. – Journal of Geophysical Research 113: G02001.

Takayanagi, H., Asami, R., Abe, O., Miyajima, T., Kitagawa, H., Sasaki, K., Iryu, Y. 2013. Intraspecific variations in carbon-isotope and oxygen-isotope compositions of a brachiopod *Basiliola lucida* collected off Okinawa-jima, southwestern Japan. – Geochimica et Cosmochimica Acta 115: 115-136.

Tintant, H. 1987. Les nautiles du Jurassique d'Arabie Saoudite. – Geobios 20, Supplement 1: 67-159.

Torsvik, T.H., van der Voo, R., Preeden, U., MacNiocaill, C., Steinberger, B., Doubrovine, P.V., van Hinsbergen, D.J.J., Domeier, M., Gaina, C., Tohver, E., Meert, J.G., McCausland, P.J.A., Cocks, L.R.M. 2012. Phanerozoic polar wander, palaeogeography and dynamics. – Earth-Science Reviews 114: 325-368.

Tynan, S., Opdyke, B.N., Walczak, M., Eggins, S., Dutton, A. 2017. Assessment of Mg/Ca in *Saccostrea glomerata* (the Sydney rock oyster) shell as a potential temperature record. – Palaeogeography, Palaeoclimatology, Palaeoecology 484: 79-88.

Ullmann, C.V., Korte, C. 2015. Diagenetic alteration in low-Mg calcite from macrofossils: a review. – Geological Quarterly 59: 3-20.

Ullmann, C.V., Campbell, H.J., Frei, R., Korte, C. 2016. Oxygen and carbon isotope and Sr/Ca signatures of high-latitude Permian to Jurassic calcite fossils from New Zealand and New Caledonia. – Gondwana Research 38: 60-73.

Urey, H.C., Lowenstam, H.A., Epstein, S., McKinney, C.R. 1951. Measurement of paleotemperatures and temperatures of the Upper Cretaceous of England, Denmark, and the southeastern United States. – Geological Society of America Bulletin 62: 399-416.

Valdes, P.J., Sellwood, B.W. 1992. A palaeoclimate model for the Kimmeridgian. – Palaeogeography, Palaeoclimatology, Palaeoecology 95: 47-72.

van Hinsbergen, D.J.J., de Groot, L.V., van Schalk, S.J., Spakman, W., Bijl, P.K., Sluijs, A., Langereis, C.G., Brinkuis, H. 2015. A paleolatitude calculator for paleoclimate studies. – PloS One 10: e0126946.

Vickers, M.L., Bajnai, D., Price, G.D., Linckens, J., Fiebig, J. 2019. Southern high-latitude warmth during the Jurassic-Cretaceous: New evidence from clumped isotope thermometry. – Geology 47: 724-728.

Vickers, M.L., Fernandez, A., Hesselbo, S.P., Price, G.D., Bernasconi, S.M., Lode, S., Ullmann, C.V., Thibault, N., Hougaard, I.W., Korte, C. 2020. Unravelling Middle to Late Jurassic palaeoceanographic and palaeoclimatic signals in the Hebrides Basin using belemnite clumped isotope thermometry. – Earth and Planetary Science Letters 546: 116401.

Wierzbowski, H. 2002. Detailed oxygen and carbon isotope stratigraphy of the Oxfordian in Central Poland. – International Journal of Earth Sciences 91: 304-314.

Wierzbowski, H. 2004. Carbon and oxygen isotope composition of Oxfordian-Early Kimmeridgian belemnite rostra: palaeoenvironmental implications for Late Jurassic seas. – Palaeogeography, Palaeoclimatology, Palaeoecology 203: 153-168.

Wierzbowski, H., Joachimski, M. 2007. Reconstruction of late Bajocian-Bathonian marine palaeoenvironments using carbon and oxygen isotope ratios of calcareous fossils from the Polish Jura Chain (central Poland). – Palaeogeography, Palaeoclimatology, Palaeoecology 254: 523-540.

Wierzbowski, H., Dembicz, K., Praszkier, T. 2009. Oxygen and carbon isotope composition of Callovian-Lower Oxfordian (Middle-Upper Jurassic) belemnite rostra from central Poland: a record of a Late Callovian global sea-level rise? – Palaeogeography, Palaeoclimatology, Palaeoecology 283: 182-194.

Wierzbowski, H., Bajnai, D., Wacker, U., Rogov, M.A., Fiebig, J., Tesakova, E.M. 2018. Clumped isotope record of salinity variations in the Subboreal Province at the Middle-Late Jurassic transition. – Global and Planetary Change 167: 172-189.

Yamano, H., Sugihara, K., Nomura, K. 2011. Rapid poleward range expansion of tropical reef corals in response to rising sea surface temperatures. – Geophysical Research Letters 38: L04601.